© 2014. Published by The Company of Biologists Ltd | Development (2014) 141, 2108-2118 doi:10.1242/dev.108118

RESEARCH ARTICLE

Co-activation of microRNAs by Zelda is essential for early *Drosophila* development

Shengbo Fu[1], Chung-Yi Nien[1], Hsiao-Lan Liang[2] and Christine Rushlow[1,*]

ABSTRACT

Transcription factors and microRNAs (miRNAs) are two important classes of *trans*-regulators in differential gene expression. Transcription factors occupy *cis*-regulatory motifs in DNA to activate or repress gene transcription, whereas miRNAs specifically pair with seed sites in target mRNAs to trigger mRNA decay or inhibit translation. Dynamic spatiotemporal expression patterns of transcription factors and miRNAs during development point to their stage- and tissue-specific functions. Recent studies have focused on miRNA functions during development; however, much remains to explore regarding how the expression of miRNAs is initiated and how dynamic miRNA expression patterns are achieved by transcriptional regulatory networks at different developmental stages. Here, we focused on the identification, regulation and function of miRNAs during the earliest stage of *Drosophila* development, when the maternal-to-zygotic transition (MZT) takes place. Eleven miRNA clusters comprise the first set of miRNAs activated in the blastoderm embryo. The transcriptional activator Zelda is required for their proper activation and regulation, and Zelda binding observed in genome-wide binding profiles is predictive of enhancer activity. In addition, other blastoderm transcription factors, comprising both activators and repressors, the activities of which are potentiated and coordinated by Zelda, contribute to the accurate temporal and spatial expression of these miRNAs, which are known to function in diverse developmental processes. Although previous genetic studies showed no early phenotypes upon loss of individual miRNAs, our analysis of the *miR-1; miR-9a* double mutant revealed defects in gastrulation, demonstrating the importance of co-activation of miRNAs by Zelda during the MZT.

KEY WORDS: MZT, Zelda, Co-activation, Gene network, MicroRNA

INTRODUCTION

Since the discovery that *lin-4* encodes a non-coding RNA (Lee et al., 1993), hundreds of microRNAs (miRNAs) have been discovered in plants, animals, single-celled eukaryotes and viruses (reviewed by Carrington and Ambros, 2003; Bartel, 2004; Kozomara and Griffiths-Jones, 2011). As inhibitors of target mRNAs, miRNAs have been shown to function in many biological processes, including development, metabolism and disease (reviewed by He and Hannon, 2004; Flynt and Lai, 2008; Mendell and Olson, 2012; Ameres and Zamore, 2013). Computational methods, classic genetic experiments and high-throughput genomic studies continue to uncover targets of miRNAs (Rajewsky, 2006; Bartel, 2009; Thomson et al., 2011). With the ever-expanding knowledge of miRNAs, their function is now seen as an important second layer of gene regulation after transcription factors in *cis-trans* regulatory networks (Martinez and Walhout, 2009), particularly since they share similar strategies in utilizing a small number of nucleotides to simultaneously regulate a large number of targets in a short time span.

The *Drosophila* model system has provided many insights into the biogenesis and functions of miRNAs. The 238 annotated miRNAs in *Drosophila* (miRBase; Kozomara and Griffiths-Jones, 2011) were identified by classic forward genetics, deep-sequencing and computational predictions (Berezikov et al., 2006, 2011; Sokol, 2008). Methods such as northern analysis, RT-qPCR and *in situ* hybridization have provided meaningful information about the level, timing and tissue-specific expression of miRNAs (Sempere et al., 2003; Aravin et al., 2003; Leaman et al., 2005; Aboobaker et al., 2005; Ruby et al., 2007).

Similar to protein-coding genes, miRNA genes are regulated by sophisticated spatial and temporal signals to ensure their proper production in specific cell types. Sokol and Ambros (2005) showed that the muscle-specific transcription factors Twist (Twi) and Mef2 are key activators of *miR-1* in *Drosophila*. Genomic studies have also identified regulators of miRNAs, such as Dorsal (Dl), c-Myc (Diminutive – FlyBase) and Ecdysone (Zeitlinger et al., 2007; Qian et al., 2011; Sempere et al., 2003). However, for many miRNAs, particularly those differentially expressed across developmental stages, the regulatory networks that control their transcription remain unknown. We are interested in the gene network that regulates miRNA functions during the maternal-to-zygotic transition (MZT), a time when developmental control is transferred from maternal products preloaded into the egg to the embryo's own genome (reviewed by Schier, 2007), which in *Drosophila* is activated ~1 hour after fertilization. During the MZT, thousands of maternal RNAs are degraded and hundreds of newly synthesized RNAs appear (Tadros and Lipshitz, 2009); thus, the MZT represents a major reprogramming event of the early transcriptome (Giraldez, 2010). Previously, we reported that the zinc-finger transcription factor Zelda (Vielfaltig – FlyBase) plays a key role during the MZT in *Drosophila*, collectively activating batteries of genes involved in early developmental processes, such as sex determination, cellularization and axis patterning (Liang et al., 2008; Nien et al., 2011). Interestingly, Zelda also activates the *miR-309* cluster of eight miRNAs (Liang et al., 2008), which is involved in the clearance of many maternally loaded mRNAs (Bushati et al., 2008). Since Zelda plays such an extensive role in zygotic genome activation, possibly as a pioneer factor to prime genes for transcriptional activation (Nien et al., 2011; Harrison et al., 2011), we investigated the possibility that Zelda activates the miRNAs expressed during the MZT.

[1]Department of Biology, New York University, 100 Washington Square East, New York, NY 10003, USA. [2]Department of Developmental and Regenerative Biology, Icahn School of Medicine at Mount Sinai, 1 Gustave L. Levy Place, New York, NY 10029, USA.

*Author for correspondence (chris.rushlow@nyu.edu)

Received 17 January 2014; Accepted 17 March 2014

Development (2014) 141, 2108-2118 doi:10.1242/dev.108118

Here, we identified a group of miRNAs (11 clusters) that are zygotically expressed in cellular blastoderm embryos, and showed that Zelda regulates all 11. We located the enhancers of several miRNAs by virtue of Zelda ChIP binding, and demonstrated that Zelda binding sites, also known as CAGGTAG sites (De Renzis et al., 2007) or TAGteam sites (Bosch et al., 2006), in these enhancers are essential for proper activation. We further showed that anteroposterior (AP) and dorsoventral (DV) patterning factors work together with Zelda to ensure timely and robust transcriptional activation of these miRNAs, contributing to their accurate spatial expression patterns. The reduced and disrupted miRNA expression seen in *zelda* mutants affects their downstream functions in maternal mRNA degradation, cell death gene repression and Hox gene regulation. We observed ventral midline defects during gastrulation in *miR-1; miR-9a* double mutants, which was not seen in either single mutant, suggesting that the coordinated activation of miRNAs by Zelda is crucial for their combinatorial function. Our analysis offers a systems-level view and understanding of the early gene network. Zelda sits as a major hub in the network, globally activating both protein-coding and non-coding genes, thereby orchestrating the early developmental processes.

RESULTS

Identification of blastoderm-expressed miRNAs by transcriptome analysis

Previous studies showed that miRNAs are expressed across different developmental stages (Aravin et al., 2003; Aboobaker et al., 2005; Ruby et al., 2007; Graveley et al., 2011). In order to focus on the set of miRNAs expressed during the MZT, and to determine which are regulated by Zelda, we examined the transcription profiles of all 188 annotated *Drosophila* miRNA loci (comprising 238 miRNAs) in our published datasets from 2- to 3-h wild-type and *zelda* mutant embryos, together with Zelda ChIP profiles (Nien et al., 2011). In total, ten loci (21 miRNAs) were expressed in 2- to 3-h embryos (Fig. 1; supplementary material Fig. S1 and Table S1). One locus is transcribed in both directions, yielding two miRNAs: miR-iab-4 and miR-iab-4as (or miR-iab-8; Ronshaugen et al., 2005; Bender, 2008; Stark et al., 2008; Tyler et al., 2008); thus, 11 miRNA clusters are transcribed in the blastoderm embryo. Strikingly, Zelda binding was observed in regions close to all of them, and most were downregulated in *zelda* mutants compared with wild type (Fig. 1; supplementary material Fig. S1 and Table S1).

Coordinated activation of early zygotic miRNAs by Zelda

We further investigated the roles of Zelda in regulating miRNAs by comparing the expression patterns of miRNAs in wild-type and *zelda* mutant embryos using *in situ* hybridization, which offers finer temporal and spatial resolution than transcriptome analysis. We designed 1-2 kb probes to target the primary miRNA (pri-miRNA) transcripts, delineated from our transcriptome data (Fig. 1; supplementary material Tables S1 and S2). For miRNAs located within introns of protein-coding genes (*miR-11* in *E2f*, *miR-92a* in *jigr1*, *miR-2a-1* in *spi*, and *miR-965* in *kis*; Fig. 1F; supplementary material Fig. S1), we used intronic sequences centered on the mature miRNA (supplementary material Tables S1 and S2). The presence of signal as nuclear dots is indicative of nascent transcripts, which distinguishes zygotic from maternal transcripts, as all four host genes are maternally loaded. Nuclear dots were observed in blastoderm embryos for all 11 miRNAs (Fig. 2). In addition, we tested the other 20 miRNAs known to be expressed in 0- to 6-h embryos (Aravin et al., 2003; Ruby et al., 2007), and, as predicted, we did not observe nuclear dots with any of these probes (supplementary material Table S1). Thus, we are confident that a total of 11 miRNA clusters are transcribed in blastoderm embryos.

Three miRNAs displayed ubiquitous expression (miR-2a-1, miR-965 and miR-309; Fig. 2A-C), whereas the remaining eight were spatially restricted along the AP or DV axes (miR-11, miR-92a, miR-92b, miR-10, miR-iab-4, miR-iab-4as, miR-1 and miR-9a; Fig. 2D-K). All 11 miRNAs were affected in *zelda* mutants, with a range of defects. Some were absent, whereas others were either reduced or became spatially modified (Fig. 2, right). In addition to these changes, we observed delays in the timing of transcriptional onset. For example, *miR-1* nascent transcripts were first detected in nuclear cycle (nc) 12 in the ventral region of the embryo (Fig. 3A, left). In *zelda* mutants, *miR-1* was not detected until nc 14, and the expression was sporadic compared with wild type (Fig. 3A-C), indicating that Zelda is required for timely and robust activation of *miR-1*.

Zelda and the patterning factors establish precise miRNA expression domains

The fact that Zelda is expressed uniformly throughout the embryo (Liang et al., 2008; Nien et al., 2011; Kanodia et al., 2012) but affects the spatially restricted miRNAs prompted us to investigate additional regulatory inputs from the AP and DV patterning factors. Two miRNAs are expressed in complementary domains along the DV axis: *miR-1* in the mesoderm and *miR-9a* in the ectoderm. Two key factors function in mesoderm specification, namely the activator Twi and the repressor Snail (Sna) (Leptin, 1991), and it is known that Twi binds and activates *miR-1* (Sokol and Ambros, 2005; Zeitlinger et al., 2007). In *zelda* mutants, *twi* activation is delayed (Nien et al., 2011), suggesting that the loss of robust expression of *miR-1* is due to both lack of direct Zelda input and reduced Twi-mediated activation.

By contrast, Sna is a likely repressor of *miR-9a* transcription in the mesoderm since it is known to inhibit the activation of many ectoderm genes (Boulay et al., 1987; Kosman et al., 1991; Leptin, 1991). Although *miR-9a* is initially ubiquitously expressed at nc 12 (data not shown), transcripts are no longer detected in the presumptive mesoderm during nc 13-14 (Fig. 3D, left), the time when the Sna protein level increases. We examined *miR-9a* in *sna* mutants and observed ectopic expression of *miR-9a* in the mesoderm (Fig. 3D, right). This repression by Sna is likely to be a direct effect, since there are four predicted Sna binding sites (ACAGGTAG, TCACCTGT, TCAGGTGG, CACCTTGC; ClusterDraw; Papatsenko, 2007) within the Zelda-bound region upstream (~7 kb) of *miR-9a*.

Repression is also the probable mechanism that regulates Hox cluster miRNAs along the AP axis (Fig. 2G-I). For example, *miR-10*, which lies between *Dfd* and *Scr* in the *Antennapedia* (*Antp*) complex, is expressed in a posterior domain (~35-85% embryo length; Fig. 2G; supplementary material Fig. S2A). In *bicoid* (*bcd*) mutant embryos, *miR-10* expression expands anteriorly to cover the entire embryo (supplementary material Fig. S2B), and when Bcd is overexpressed, as in 6× *bcd* embryos (Ochoa-Espinosa et al., 2009), *miR-10* expression moves posteriorly and becomes restricted to ~60-85% of the embryo length (supplementary material Fig. S2C). Thus, activation by Zelda and repression by Bcd-dependent anterior repressors set the *miR-10* domain. One such repressor is possibly Hunchback (Hb), since it acts mainly as a repressor of posterior gap genes in the anterior region, and its expression domain is complementary to that of *miR-10* (Hülskamp et al., 1990). Similarly, *miR-iab-4* and *miR-iab-4as*, which are expressed posteriorly (Fig. 2H,I), are derepressed in the head region of *bcd* mutants (data not shown).

Development (2014) 141, 2108-2118 doi:10.1242/dev.108118

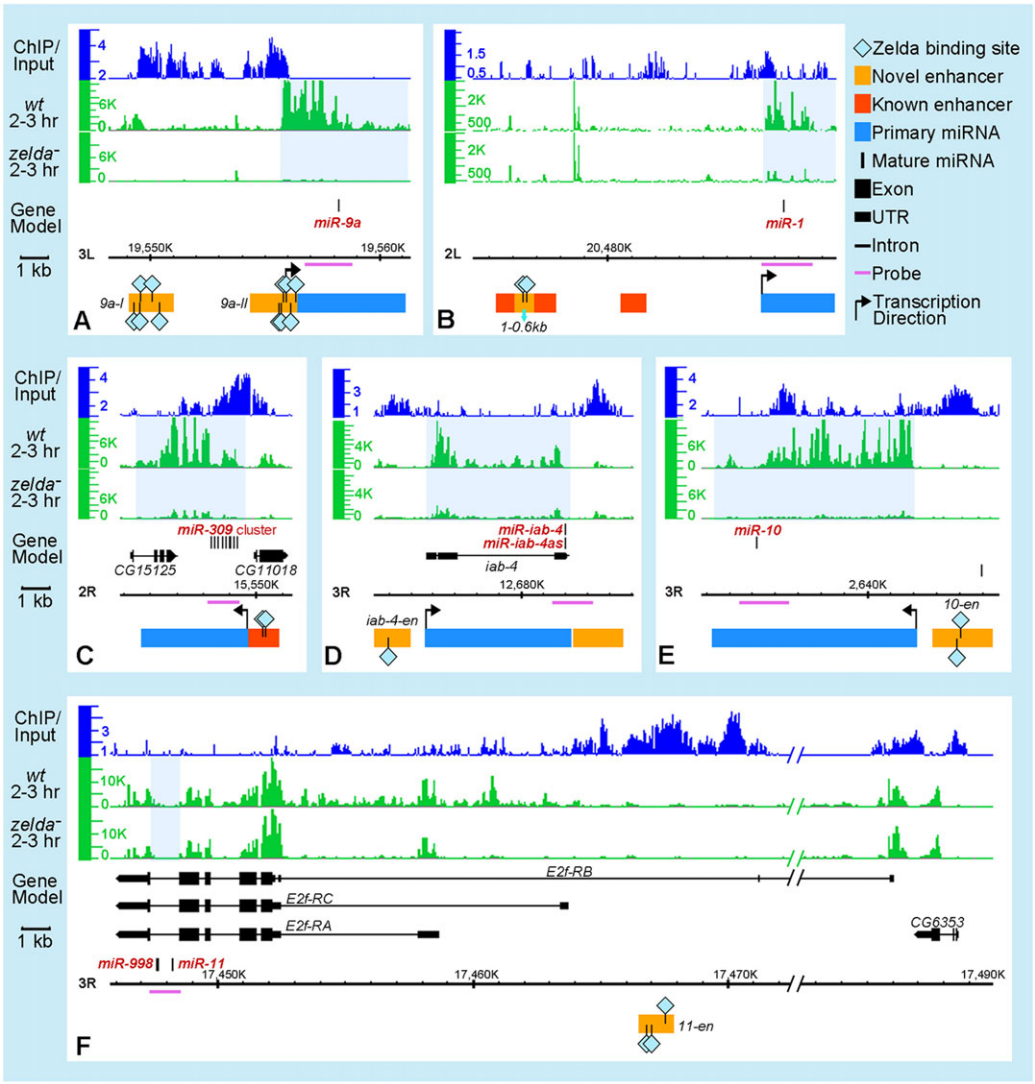

Fig. 1. Zelda binds upstream of miRNA transcription units and regulates their expression. Integrated Genome Browser (IGB) (Nicol et al., 2009) views are shown for six *Drosophila* miRNA loci (A-F; miRNAs shown as black vertical lines in the gene model; genome version BDGP R5/dm3). Tracks above gene models represent data from Nien et al. (Nien et al., 2011) as follows: Zelda ChIP binding in 1- to 2-h wild-type (*wt*) embryos (top, blue), RNA expression profiles of 2- to 3-h *wt* (middle, green) and *zelda* mutant (bottom, green) embryos. Highlighted below the gene models are: pri-miRNA transcription units (blue rectangles) estimated from the *wt* expression track, previously identified miRNA enhancers (red boxes) (Biemar et al., 2005; Zeitlinger et al., 2007), and newly identified enhancers from this study (orange boxes). Zelda binding sites (light blue diamonds) within enhancers are indicated. The horizontal purple lines under the gene models delineate the probes used to detect pri-miRNA transcripts in embryos. Light blue shading on the expression tracks indicates intergenic or intronic regions harboring the miRNAs that are downregulated in *zelda* mutants. Note that *miR-11* is located within an intron of the *E2f-RC* isoform (F), and Zelda-bound regions lie upstream of *E2f-RB*.

Taken together, these results suggest that repressor activity is essential to prevent the expression of Hox cluster miRNAs in anterior regions. Given that these miRNAs are involved in regulating other Hox genes (Ronshaugen et al., 2005; Bender, 2008; Stark et al., 2008; Tyler et al., 2008; Gummalla et al., 2012), it is important that their borders of expression are precisely established. This is achieved by the coordinated activity of uniformly distributed Zelda and spatially localized AP repressors.

Interestingly, *miR-iab-4* and *miR-iab-4as* are transcribed from opposite strands of the same locus (Ronshaugen et al., 2005; Bender, 2008; Stark et al., 2008; Tyler et al., 2008), but they are regulated differently. Although both are expressed posteriorly, *miR-iab-4* is much broader, and in *zelda* mutants *miR-iab-4* disappears, whereas *miR-iab-4as* expands anteriorly (compare Fig. 2H,I). Zelda is likely to regulate *miR-iab-4as* indirectly by ensuring the proper localization of AP repressors. It is known that in *zelda* mutants, the gap gene repressor domains shift and/or expand (Nien et al., 2011), which results in a cascade effect on downstream targets including miRNAs.

Patterning factors also contribute to ubiquitously expressed miRNAs

We expected to see the ubiquitously expressed *miR-309* transcripts disappear in *zelda* mutants, but they persisted in the anterior region, in an *hb*-like domain (Fig. 2C). In the absence of Bcd, *miR-309* is initially ubiquitous as in wild type, indicating that the onset of *miR-309* expression is mediated by Zelda; however, shortly thereafter, transcripts are lost anteriorly (supplementary material Fig. S3A,B), probably owing to the lack of Bcd-dependent activation. In addition, both Zelda and Bcd exert regulatory activity on the known *miR-309*

Development (2014) 141, 2108-2118 doi:10.1242/dev.108118

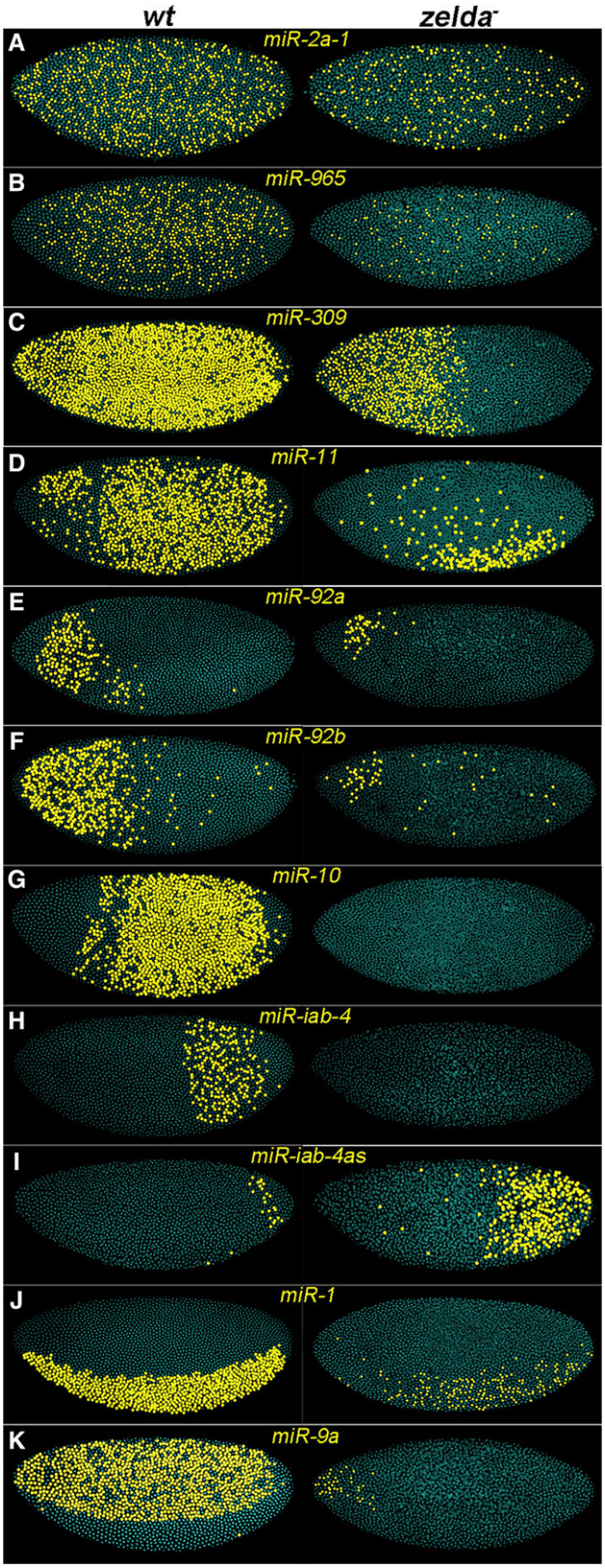

Fig. 2. Zelda is required for proper miRNA activation. Pseudocolored confocal FISH images (see Materials and Methods) of wild-type (*wt*, left) and *zelda* mutant (right) embryos hybridized with RNA probes against pri-miRNAs (A-K, as indicated). Yellow dots represent nuclei with nascent transcripts. Embryos are oriented anterior to the left and dorsal up. Pri-miRNAs show diverse expression patterns in *wt* embryos, and these are affected in *zelda* mutants.

enhancer region. This enhancer drives the expression of a *lacZ* reporter gene in a similar pattern to endogenous *miR-309* (supplementary material Fig. S3C) (Biemar et al., 2005). In the absence of Zelda, *lacZ* is only expressed in the anterior region (supplementary material Fig. S3D), resembling the endogenous expression pattern of *miR-309* in *zelda* mutants (Fig. 2C, right). In the absence of Bcd, *lacZ* expression is decreased in the anterior region at the blastoderm stage, and later becomes restricted posteriorly (supplementary material Fig. S3E). These observations suggest that the uniform *miR-309* pattern is composed of multiple overlapping patterns regulated by the combinatorial action of Zelda and Bcd-dependent factors. This type of multifactor regulation is also seen for *miR-11*, the expression of which is observed in a discrete ventral domain in the absence of Zelda (Fig. 2D).

Using Zelda binding profiles to locate miRNA enhancers

Previous studies have shown that Zelda binds to enhancers of many known blastoderm-expressed genes (Nien et al., 2011; Harrison et al., 2011); hence, we hypothesized that enhancers of early miRNAs could be located by searching for Zelda-bound regions close to miRNA transcription units. First, we noticed that Zelda binds to previously defined enhancers of *miR-1* (Zeitlinger et al., 2007) and *miR-309* (Biemar et al., 2005) (red rectangles in Fig. 1B,C). Next, we tested Zelda-bound regions that lie upstream of the *miR-10*, *miR-iab-4*, *miR-11*, *miR-9a* and *miR-92a* transcription units (see Fig. 1) in transgenic reporter assays. Reporter gene expression recapitulated endogenous miRNA expression in all but one case, *miR-92a*, for which the tested fragment directed a different pattern and could be the enhancer of a nearby gene (Fig. 4A-C and Fig. 5C; data not shown for *miR-92a*). These results suggest that Zelda binding can be used to pinpoint bona fide enhancers of early miRNAs.

Interestingly, *miR-11* resides in the fifth intron of the *RC* isoform of the *E2f* gene (see Fig. 1F), which is the isoform present in blastoderm embryos. Because *E2f* is maternally supplied (Thomsen et al., 2010), zygotic transcripts can be distinguished only by detecting hybridization signal over introns, which is clearly reduced in *zelda* mutants, whereas the *E2f* exonic signal appears little affected (Fig. 1F). These results are consistent with the idea that Zelda regulates zygotic activation of the *E2f-RC* isoform, and therefore *miR-11*.

In our search for *miR-9a* enhancers, we tested two fragments, *9a-I* and *9a-II* (Fig. 1A), both of which drove *lacZ* in a *miR-9a*-like ectodermal pattern that was lost in the absence of Zelda (Fig. 5C,D; data not shown for *9a-I*). However, the *9a-I* enhancer gave a somewhat stripey pattern along the AP axis (data not shown). Although not fully redundant, both enhancers might be required for robust and accurate expression of *miR-9a*, as has been shown for the primary and shadow enhancers of *sna* and *hb* (Perry et al., 2010, 2011).

Zelda binding sites in the *miR-1* and *miR-9a* enhancers are required for proper expression

To demonstrate that Zelda binding sites in the miRNA enhancers are essential for activation, we mutated the sites in the *miR-9a-II* and *miR-1* enhancers. The *miR-9a-II* enhancer contains six Zelda binding sites. Mutation of the two distalmost Zelda binding sites (*9a-IIm1*) resulted in loss of *lacZ* expression except in the head region (Fig. 5E), which is similar to endogenous *miR-9a* expression in *zelda* mutants (Fig. 5B). Mutation of the middle two Zelda binding sites caused a similar effect (Fig. 5F), indicating that both sets of sites are required for transcriptional activation.

For *miR-1*, we further dissected the known enhancer identified by Zeitlinger et al. (Zeitlinger et al., 2007), which was located by virtue

Development (2014) 141, 2108-2118 doi:10.1242/dev.108118

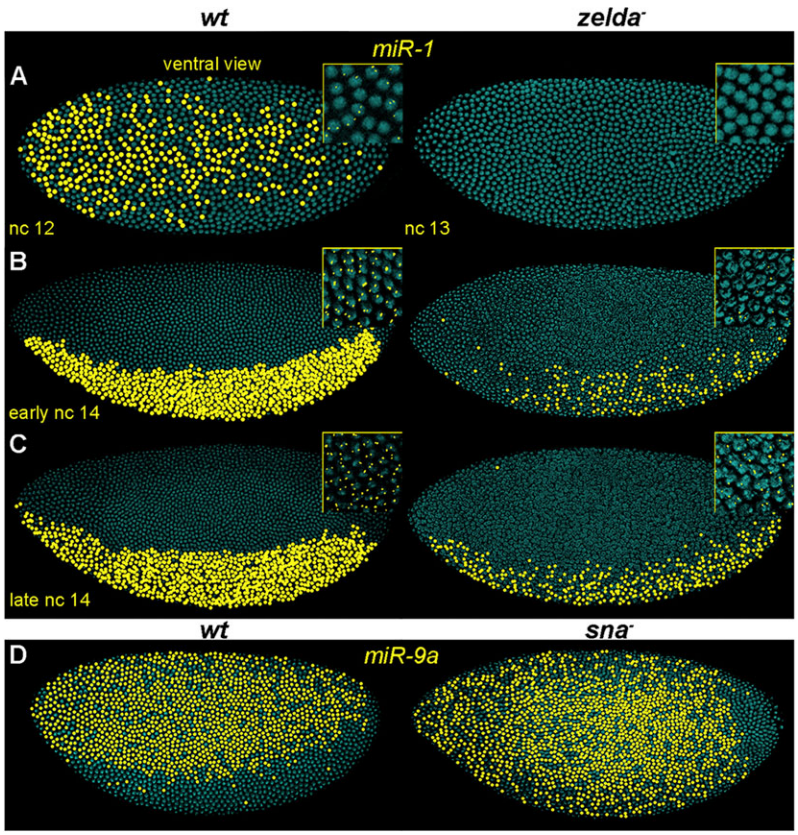

Fig. 3. Patterning factors spatially regulate miRNA expression. Pseudocolored confocal FISH images of embryos hybridized with *pri-miR-1* (A-C) or *pri-miR-9a* (D) probes. (A-C) Wild-type (left) and *zelda* mutant (right) embryos; insets show the actual FISH signal localized in nuclei. Note that the expression of *miR-1* was first detected in nuclear cycle (nc) 12 in *wt* (A, left), but was not detected until early nc 14 in *zelda* mutants and the expression was also less robust (B, right). (D) *miR-9a* expression expands ventrally in *sna* mutants (right), indicating that Sna represses *miR-9a* in the presumptive mesoderm.

of Twi and Dl binding profiles. An internal 0.6 kb fragment that contains two Zelda binding sites directed a ventral *miR-1*-like pattern (Fig. 5G,H), which was lost in the *zelda* mutant background (Fig. 5I). Mutation of the first or second binding site, or both, caused reduced *lacZ* expression (Fig. 5J-L), indicating that both sites are important for *miR-1* activation in blastoderm embryos. We also examined reporter gene expression in older embryos, since *miR-1* is expressed throughout the mesodermal tissue in stage 10 embryos (Aboobaker et al., 2005). All four reporters directed late expression, including the mutated forms (data not shown), demonstrating that *miR-1* expression at stage 10 is not regulated by Zelda.

Zelda-activated miRNAs function in diverse processes during the MZT

Our results show that Zelda is central to the miRNA early transcription network, ensuring the timely, robust and spatially precise activation of miRNAs, which in turn might be important for the proper inhibition of their targets. Since activation of all but one miRNA is substantially downregulated in *zelda* mutants, we reasoned that downstream targets of miRNAs might be included in the set of transcripts upregulated in *zelda* mutants. Indeed, several genes in this set have previously been verified as targets of miRNAs including miR-309 (Bushati et al., 2008), miR-11 and the miR-2 family (Leaman et al., 2005), and miR-iab-4/4as (Ronshaugen et al., 2005; Bender, 2008; Stark et al., 2008; Tyler et al., 2008).

The miR-309 cluster of miRNAs mediates the degradation of ~138 maternally loaded RNAs (Bushati et al., 2008). In the absence of Zelda, 774 genes were upregulated in 2- to 3-h embryos (Nien et al., 2011), and 534 (61.6%) of these can be classified as unstable maternal mRNAs (supplementary material Table S3 and Fig. S4) (Thomsen et al., 2010) and thus represent mRNAs that are normally degraded in wild type, but persist in *zelda* mutants during the MZT. Degradation of 434 (81%) of these unstable maternal mRNAs depends on zygotically derived factors (Thomsen et al., 2010), 125 of which are upregulated in *miR-309* mutants (Bushati et al., 2008). Importantly, of 29 experimentally verified miR-309 targets (Bushati et al., 2008), 15 are significantly upregulated in *zelda* mutants (supplementary material Table S3). One possible reason that not all

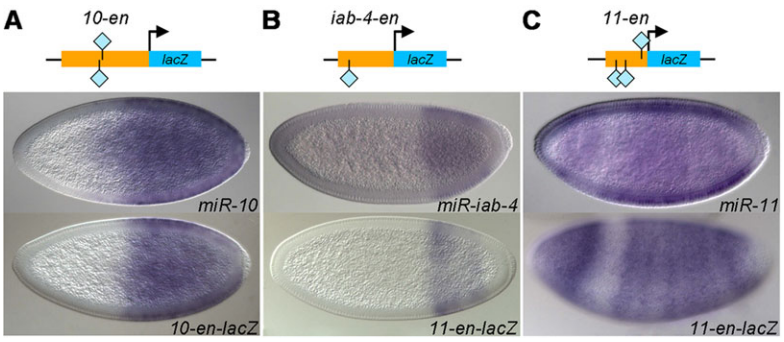

Fig. 4. Identification of novel enhancers of miRNAs. (Above) Schematic representation of the transgenic constructs, with enhancer fragments (orange rectangles) from *miR-10* (A), *miR-iab-4* (B) and *miR-11* (C) fused to a *lacZ* reporter (blue rectangles). Light blue diamond represents Zelda binding site. (Below) Reporter expression (bottom row of embryos) recapitulates the endogenous miRNA pattern (top row of embryos).

Development (2014) 141, 2108-2118 doi:10.1242/dev.108118

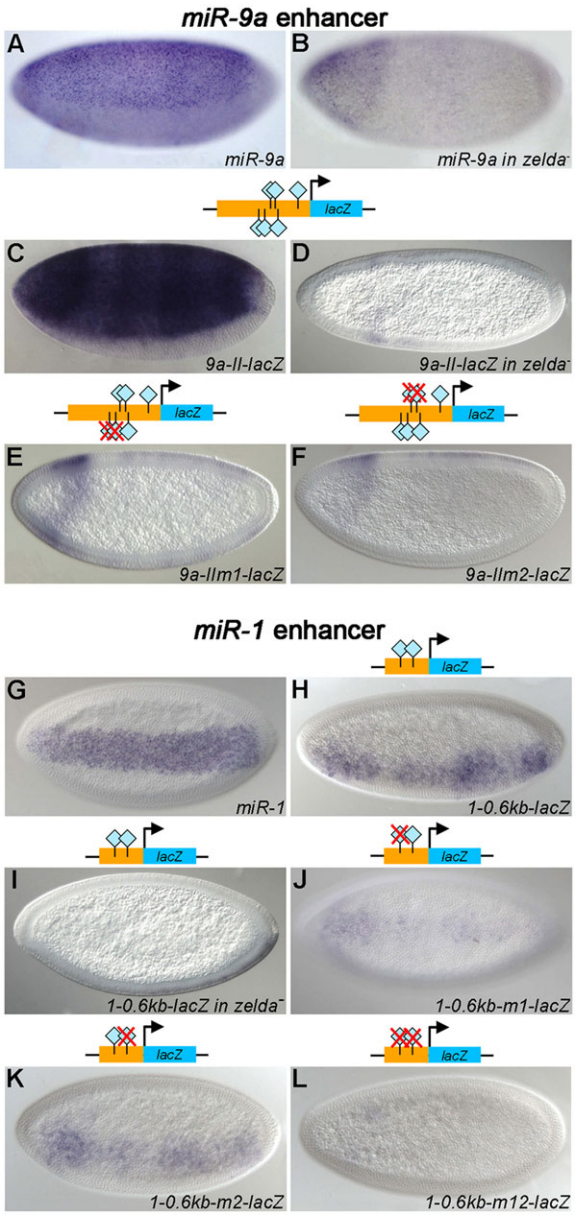

Fig. 5. Zelda binding sites in miRNA enhancers are crucial for transcriptional activation. Embryos were hybridized with RNA probes against *pri-miR-9a* (A,B), *pri-miR-1* (G) or *lacZ* (C-F,H-L). Embryos are in lateral (A-F) or ventral/ventrolateral (G-L) view. Transgenic embryos carry wild-type or mutated versions (red Xs) of the *miR-9a* (C-F) and *miR-1* (I-L) enhancers (see genomic locations in Fig. 1). Mutation of Zelda binding sites affected reporter expression in all cases (E,F,J-L), indicating that Zelda activates *miR-9a* and *miR-1* directly by binding to their enhancers.

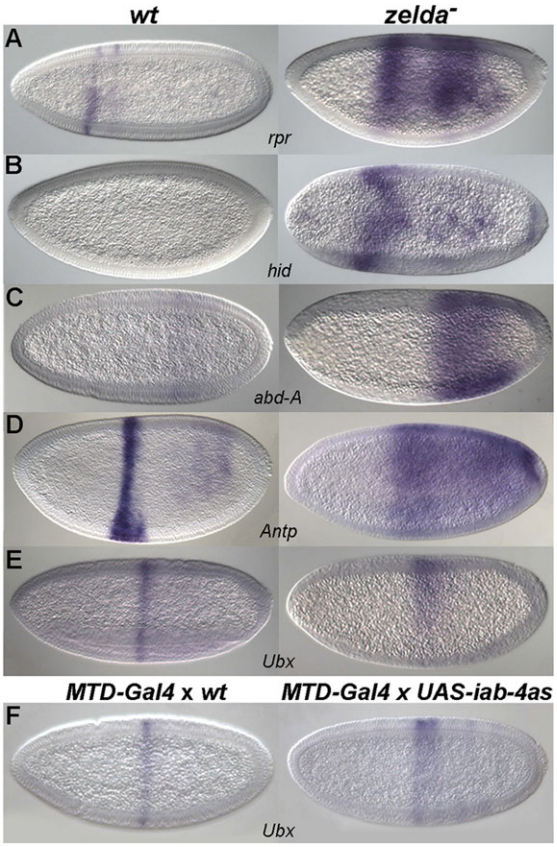

Fig. 6. miRNA target expression is affected in *zelda* mutants. Wild-type (left) and *zelda* mutant (right) embryos were hybridized with RNA probes as indicated. Expression of miRNA targets *rpr* (A), *hid* (B), *abd-A* (C), *Antp* (D) and *Ubx* (E) is upregulated in *zelda* mutants. The posterior expansion of *Ubx* (E) in *zelda* mutants is partially due to the upregulation of *miR-iab-4as* (see Fig. 2I), since a similar effect was observed when *miR-iab-4as* was ectopically expressed (F, right).

of the genes upregulated in *miR-309* mutants were upregulated in *zelda* mutants could relate to the residual anterior miR-309 function in *zelda* mutants (Fig. 2C, right).

Besides maternal genes, the upregulated genes in *zelda* mutants also include zygotic genes, some of which are also verified miRNA targets. For example, two key regulators of *Drosophila* programmed cell death, *reaper* (*rpr*) and *head involution defective* (*hid*, also known as *Wrinkled*), were upregulated in *zelda* mutants (by >1.5-fold, $P<0.05$; supplementary material Table S3; Fig. 6A,B). Both *rpr* and *hid* are verified targets of miR-11, miR-2 and of miR-6, which is a member of the miR-309 complex, in mid-stage embryos (Leaman et al., 2005; Truscott et al., 2011; Ge et al., 2012).

In early wild-type embryos, *rpr* is expressed in two stripes in the anterior region (Fig. 6A), in a domain complementary to that of *miR-11* (Fig. 2D and Fig. 4C). In *zelda* mutants, *rpr* is ectopically expressed posteriorly, except in the ventral region (Fig. 6A) where *miR-11* remains (Fig. 2D), indicating that miR-11 might directly regulate *rpr* in blastoderm embryos as it does in older embryos. *hid* transcripts are not normally observed before gastrulation, but appear earlier in *zelda* mutants (Fig. 6B).

Other examples of zygotic genes targeted by early miRNAs include Hox genes. *abd-A* is a direct target of miR-iab-4as (Bender, 2008; Gummalla et al., 2012), and *Ubx* was verified to be a target of both miR-iab-4 and miR-iab-4as (Ronshaugen et al., 2005; Bender, 2008; Stark et al., 2008; Tyler et al., 2008). *Antp* is predicted to be a target of miR-iab-4 and miR-iab-4as (TargetScanFly; Ruby et al., 2007). Interestingly, *abd-A*, *Ubx* and *Antp* are all upregulated in *zelda* mutant embryos, and their expression domains expand posteriorly (Fig. 6C-E; supplementary material Table S3 and Fig. S5), which might in part be due to the misregulation of miRNA activity in posterior regions (Fig. 2H,I). One piece of evidence to support this idea is the posterior expansion of *Ubx* when *miR-iab-4as* is ectopically expressed (Fig. 6F; see Materials and Methods), an effect also seen in *zelda* mutants (Fig. 6E).

Spatially restricted expression of Hox genes relies on multiple regulatory inputs (reviewed by McGinnis and Krumlauf, 1992; Gellon and McGinnis, 1998; Yekta et al., 2008), including cross-regulation

Development (2014) 141, 2108-2118 doi:10.1242/dev.108118

among Hox genes, particularly 'posterior prevalence', whereby the posterior Hox genes repress the more anterior ones. Interestingly, the miRNAs embedded in the Hox complexes follow this rule, as they repress Hox genes expressed more anteriorly (Yekta et al., 2008). Finally, long intergenic non-coding RNAs (lincRNAs) transcribed from the Hox complexes have recently been identified as regulators of Hox genes by interfering with their transcription; for example, *bithoraxoid* (*bxd*) RNAs repress *Ubx* (Petruk et al., 2006), whereas the iab-8 RNAs, comprising lincRNA and miR-iab-4as, repress *abd-A* (Gummalla et al., 2012). The expression level of *bxd* is downregulated in *zelda* mutant embryos (blue shading in supplementary material Fig. S5A), which might also contribute to the derepression of *Ubx* in the absence of Zelda. Transcription in the *iab-8* region is upregulated in *zelda* mutants (red shading in supplementary material Fig. S5A), but how this affects *abd-A* regulation is complicated by the presence of other non-coding RNAs within the long, 92 kb *iab-8* transcript, including *iab-4* and *CR43617* (supplementary material Fig. S5A) (FlyBase; Tweedie et al., 2009), which are downregulated in *zelda* mutants (blue shading in supplementary material Fig. S5A). In the *Antp* complex, *CR44931*, a lincRNA that lies between *ftz* and *Antp*, is absent in *zelda* mutants (blue shading in supplementary material Fig. S5B). Thus, Zelda regulation of the Hox genes is multilayered, involving miRNAs and lincRNAs, as well as indirect effects on the upstream patterning factors in the segmentation hierarchy that regulates transcription of the Hox genes (Nien et al., 2011).

Co-activation of miRNAs by Zelda is crucial for normal development

So far, our results indicate that Zelda coordinately activates a set of miRNAs, and in turn these miRNAs inhibit sets of downstream target RNAs. One question is whether it is significant that these particular miRNAs are co-expressed together in the blastoderm embryo. Of the early expressed miRNAs, loss-of-function mutations have been made in *miR-309* (Bushati et al., 2008) as mentioned above, *miR-1* (Sokol and Ambros, 2005), *miR-9a* (Li et al., 2006), *miR-11* (Truscott et al., 2011), *miR-iab-4/4as* (Bender, 2008), *miR-10* (Lemons et al., 2012) and *miR-92a* (Chen et al., 2012b). Curiously, none of these mutants displayed early morphological phenotypes despite the fact that miRNA targets for some were identified and verified. In most cases, mutants survived to adulthood, suggesting that, individually, these miRNAs have subtle effects at best. However, as previously noted by many investigators, miRNAs often function redundantly or have small contributions by themselves (reviewed by Smibert and Lai, 2008). Hence, knocking out combinations of miRNAs may have more dramatic effects. For example, Ge et al. (Ge et al., 2012) reported that the *miR-6; miR-11* double mutant exhibits a strong reduction in survival to adulthood compared with either of the single mutants, and that this phenotype was due to elevated apoptosis activity as a result of decreased degradation of the targets *rpr* and *hid* in mid-stage embryos.

To further study the significance of the coordinated expression of miRNAs, we examined embryos doubly mutant for *miR-1* and *miR-9a*, which are directly regulated by Zelda (Fig. 5). The double mutants are embryonic lethal and display gastrulation defects during ventral furrow formation (Fig. 7B, arrows; data not shown). Normally, *rhomboid* (*rho*), a component of EGFR signaling, is expressed in ventrolateral stripes in the blastoderm (Fig. 7A, left), which refine and then progressively meet at the ventral midline as the ventral furrow invaginates (Fig. 7B,C, left). Later, the *rho*-labeled cells form a single straight stripe along the ventral midline that persists through germband extension, marking the mesectoderm (Fig. 7D,E, left). In the *miR-1; miR-9a* double mutant, the progression of ventral-midline closure is

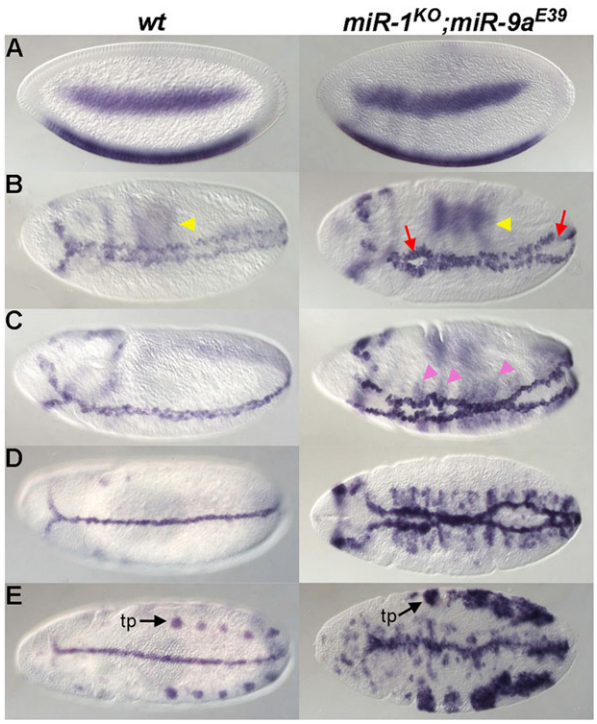

Fig. 7. *miR-1; miR-9a* double mutants display ventral midline defects. Wild-type (left) and *miR-1; miR-9a* double-mutant (right) embryos of increasing age (A-E) were hybridized with *rho* probes. Yellow arrowheads in B indicate dorsal expression of *rho*. In the nc 14 embryo (A), *rho* expression is detected in two ventrolateral stripes, which come together during ventral furrow formation in stage 8-10 embryos (B-D), forming the ventral midline. *rho* is expressed in tracheal pits (tp, black arrows) after stage 11 (E). *miR-1; miR-9a* double-mutant embryos are defective in synchronized ventral midline closure, as anterior and posterior gaps are visible (B, red arrows). Ectopic *rho* expression is observed along the midline (C, pink arrowheads).

desynchronized, with lagging gaps, eventually forming a disorganized midline (Fig. 7B, red arrows). In addition, ectopic expression of *rho* was observed in cells adjacent to midline cells (Fig. 7C, pink arrowheads), and the organization of *rho*-expressing cells in the tracheal pits is also abnormal, as shown by the larger clumps of *rho*-expressing cells (Fig. 7E, right, black arrow) and the lack of even spacing between the pits. These phenotypes were not observed in either of the two single mutants (data not shown), suggesting that proper gastrulation movements require the combined activity of the *miR-1* and *miR-9a* miRNAs. Although *miR-1* is expressed in the mesoderm and *miR-9a* in the ectoderm (Fig. 2J,K), they might influence signaling at the boundary where the mesectoderm forms.

DISCUSSION

In this study we identified the set of miRNAs expressed in 2- to 3-h *Drosophila* embryos, a time when the MZT is well underway and the fate map of the embryo is being established (Figs 1 and 2; supplementary material Fig. S1). These early expressed miRNAs are regulated globally by Zelda, both directly via binding to *cis*-regulatory enhancers and indirectly by affecting the expression of additional transcriptional regulators (Figs 2-5; supplementary material Figs S2 and S3). Together with previously published data on specific miRNAs, we were able to integrate the early miRNAs, their upstream regulators and downstream targets into the early gene network (Fig. 8). In addition, our results emphasize the importance of co-activation of miRNAs by Zelda, which ensures their combined activity.

Development (2014) 141, 2108-2118 doi:10.1242/dev.108118

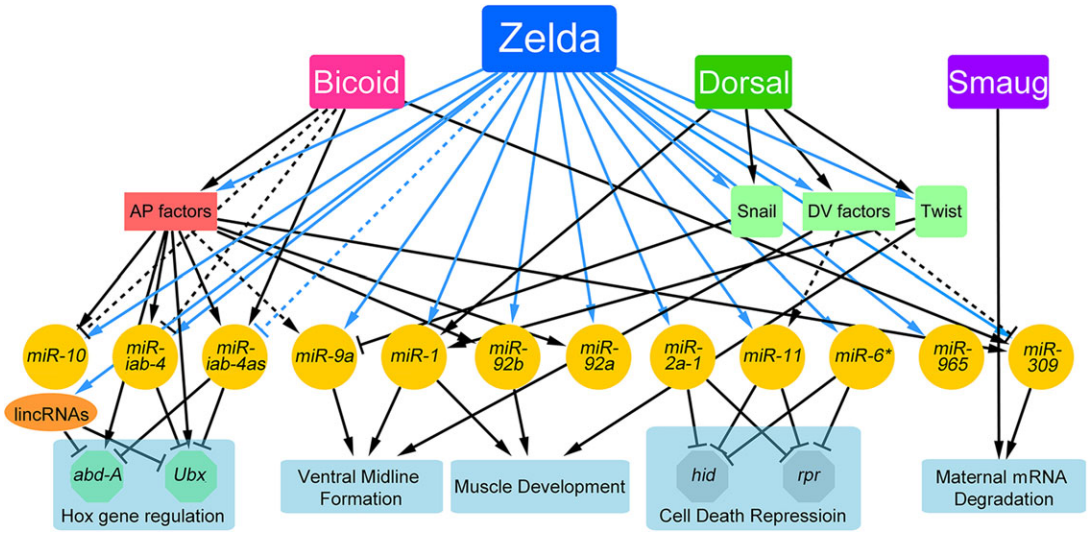

Fig. 8. miRNAs complete the early gene network. Protein-coding genes and miRNAs are nodes in this network. Arrows indicate positive regulation (transcriptional activation or promotion); T bar represents negative regulation (transcriptional repression, or repression/destabilization via the 3′UTR); and dashed lines indicate putative connections. Zelda is a central hub in the early gene regulatory network (Nien et al., 2011), working together with maternal morphogens and newly transcribed zygotic transcription factors to ensure accurate spatial and temporal expression of miRNAs. Zelda links the interplay between miRNAs and transcription factors by regulating the transcription of both. **miR-6* is one of the eight miRNAs in the *miR-309* cluster.

Zelda activates the blastoderm-specific miRNAs

Using our expression profiling data from 2- to 3-h wild-type and *zelda* mutant embryos (Nien et al., 2011), we identified blastoderm-specific pri-miRNA transcription units, which included seven intergenic and four intronic miRNAs (clusters) (Fig. 1; supplementary material Fig. S1). Since the expression levels of all 11 miRNAs were affected in *zelda* mutants (Fig. 2), we were able to better distinguish blastoderm-specific isoforms, particularly in the case of intronic miRNAs, such as *miR-11*, which resides in an intron of *E2f* (Fig. 1F). Moreover, maternal *E2f* expression could be differentiated from zygotic expression by observing the intronic signal, which was clearly downregulated in *zelda* mutants (Fig. 1F).

Precise miRNA expression patterns are established by the early gene network

The early miRNAs exhibit strikingly different expression patterns (Fig. 2), and it is noteworthy that, similar to the protein-coding targets of Zelda, two different strategies are used to regulate these miRNAs. Some miRNAs, such as *miR-9a*, were completely abolished in *zelda* mutants, indicating that Zelda is their sole activator, whereas others, such as *miR-1*, were affected temporally and/or spatially (Fig. 2J and Fig. 3A-C), indicating that Zelda works together with other factors to establish robust and precise domains of expression. For example, *miR-1* downregulation in *zelda* mutants is likely to be due to the cumulative effect of loss of direct inputs from Zelda and the delayed expression of *twi* that occurs in *zelda* mutants (Nien et al., 2011). Thus, the effect on *miR-1* is the result of a breakdown in the Zelda-Twi-miR-1 feedforward loop (Fig. 8).

Zelda binding marks miRNA enhancers

Cis-regulatory modules/enhancers of miRNAs have been predicted based on the presence of transcription factor binding (Zeitlinger et al., 2007; The modENCODE Consortium et al., 2010) or specific chromatin marks (Ozsolak et al., 2008), and verified in only some cases. For example, two regions upstream of *miR-1* that bind Twi/Dl were shown to drive a *miR-1*-like expression pattern (Zeitlinger et al., 2007). We reasoned that we could locate enhancers of all early miRNAs by simply looking for Zelda-bound regions upstream of the pri-miRNA transcription units, especially since Zelda is a global activator during the MZT. This approach worked well; eight of nine enhancers recapitulated endogenous-like expression (Figs 4 and 5). Mutation of Zelda binding sites in enhancers further demonstrated direct Zelda input. As proof of principle, we assayed enhancers of two genes, *miR-9a* and *miR-1*, and showed that mutation of the Zelda binding sites had the same effect as eliminating Zelda in *trans* (Fig. 5). These results indicate that Zelda directly regulates the early expressed miRNAs, often in conjunction with other transcription factors, many of which are also regulated by Zelda (Nien et al., 2011). Zelda is a major hub in the early network, establishing multiple feedforward loops and closely linking the transcription factors and miRNAs expressed in this stage (Fig. 8).

Zelda plays important roles in both hallmark events of the MZT

The MZT is a key event during the development of an organism, whereby the transcriptome is reprogrammed in the first few hours of development. This requires the clearance of previous information (maternal mRNA degradation) and the initiation of a new program (zygotic genome activation). The maternal mRNA degradation machinery comprises both maternally derived and zygotically derived pathways (Bashirullah et al., 1999; Tadros and Lipshitz, 2009). In *Drosophila*, Smaug (Smg), a maternally loaded RNA-binding protein, is central to the mRNA clearance pathway. By recruiting the CCR4-NOT deadenylation complex, Smg destabilizes two-thirds of the maternal mRNAs that undergo degradation (i.e. that are unstable) upon egg activation (Tadros et al., 2007). By contrast, miR-309 is a key component of the zygotically derived pathway to clear mRNAs (Bushati et al., 2008). When analyzing the maternal RNAs upregulated in *zelda* mutants, we noted that 81% of them (434) depend on zygotic degradation pathways (supplementary material Fig. S4B); 125 of the 434 genes are also upregulated in *miR-309* mutants (Bushati et al., 2008) (supplementary material Fig. S4C), indicating that Zelda, by activating *miR-309*, is involved in maternal RNA degradation (Fig. 8). Therefore, Zelda plays important roles in both of the hallmark events of the MZT. Interestingly, the miR-309 targets

Development (2014) 141, 2108-2118 doi:10.1242/dev.108118

account for only ~30% of the unstable maternal RNAs upregulated in *zelda* mutants (supplementary material Fig. S4B, classes III and IV), and another 14% are putative targets of the other early miRNAs, indicating that Zelda might activate additional zygotic pathways to mediate maternal mRNA degradation.

Coordinated miRNA activation by Zelda is important for *in vivo* function

Several miRNAs, in addition to miR-309, have been shown to target specific mRNAs in the early embryo; for example, miR-iab-4 and miR-iab-4as target Hox genes (Ronshaugen et al., 2005; Bender, 2008; Stark et al., 2008; Tyler et al., 2008). However, although each of the miRNAs is predicted to target hundreds of genes (Bartel, 2009), in many cases the individual miRNA loss-of-function phenotypes are relatively mild (reviewed by Smibert and Lai, 2008). There are several explanations for this phenomenon: (1) the miRNA does not function at the time that it is expressed, but might function later; (2) miRNAs 'fine-tune' the expression levels of their target genes, which might not be reflected in obvious phenotypes when they are mutated; and (3) miRNA functions are redundant, such that knockdown of one miRNA may be compensated by another.

To better address the functions of miRNAs, investigators have used several genetic approaches: gain-of-function assays (Bejarano et al., 2012), using sensitized genetic backgrounds (Brenner et al., 2010), and assaying double mutants (Ge et al., 2012). For example, the *miR-6; miR-11* double mutant exhibits increased apoptosis, leading to lower survival rates compared with either of the single miRNA mutants (Ge et al., 2012). Using a similar approach, we observed fully penetrant gastrulation defects in *miR-1; miR-9a* double mutants (Fig. 7). Neither single mutant is embryonic lethal, nor shows any sign of ventral furrow defects; however, *miR-1* mutants are larval lethal and display muscle defects (Sokol and Ambros, 2005), while *miR-9a* mutants show wing margin defects in adulthood (Li et al., 2006). Importantly, the double-mutant phenotype is the earliest phenotype seen for any known miRNA, or combination of miRNAs, thus far tested. These results support the idea that co-activation of miRNAs by Zelda is required for normal development.

The *miR-1; miR-9a* double-mutant phenotype resembles, to some extent, the ventral furrow defects observed in *RhoGEF2* loss-of-function mutants (Barrett et al., 1997). Rho signaling is involved in the cell shape changes associated with ventral furrow invagination, and loss of Rho signaling results in very disorganized invagination (Barrett et al., 1997). Curiously, miR-1 and miR-9a are both predicted to target *RhoGAP68F*, a negative regulator of Rho signaling (Sanny et al., 2006). *RhoGAP68F* is maternally loaded and cleared during the MZT (Thomsen et al., 2010). It is possible that the gastrulation phenotype of the *miR-1; miR-9a* double mutant is caused in part by excess activity of RhoGAP68F. Although we did not see any obvious upregulation of *RhoGAP68F* transcripts in *miR-1; miR-9a* mutant embryos by *in situ* hybridization (data not shown), it is possible that subtle upregulation of *RhoGAP68F*, combined with effects on other predicted targets, all contribute to the gastrulation defects observed in the double mutant.

The co-activation of groups of miRNAs by master regulators such as Zelda may be crucial for miRNA activity during development, as revealed by the severe gastrulation phenotype of the *miR-1; miR-9a* double mutant. Such coordinated activation of miRNAs might also occur at later stages in development in tissues in which Zelda is expressed, such as the central nervous system (Liang et al., 2008). In the future, various combinations of mutations in miRNA genes that are co-regulated by Zelda, or other key factors, might unveil additional functions of miRNAs across development stages.

MATERIALS AND METHODS

Drosophila genetics

The $y^1 w^{67c23}$ strain was used as wild-type (*wt*) control. The zld^{294} allele was used to obtain *zelda* germline clones as previously described (Liang et al., 2008). Other alleles used include bcd^{E1}, sna^1, gd^7 and MTD-*gal4* (31777, Bloomington *Drosophila* Stock Center). bcd^{+5} bcd^{+8}/bcd^{+5} bcd^{+8}; vas^{PD} exu^{PJ}/vas^{PD} exu^{PJ} (6× *bcd*; Ochoa-Espinosa et al., 2009) was used to overexpress Bcd. *P{attP.w+.attP} JB38F* (38F1; 27388, Bloomington *Drosophila* Stock Center) was used for transgene injection. The *UAS-miRNA* fly lines were generously supplied by Eric Lai (Bejarano et al., 2012). *miR-1; miR-9a* double mutants were obtained by crossing $miR\text{-}1^{KO}$/*SM6B, eve-lacZ* (Sokol and Ambros, 2005) and $miR\text{-}9a^{E39}$/*TM3B, hb-lacZ* (Li et al., 2006) flies. Homozygous *miR-1; miR-9a* double-mutant embryos were identified by the absence of *lacZ* expression.

Mutagenesis and enhancer testing

Candidate enhancer fragments were chosen by identifying regions near transcription units of miRNAs that overlapped with Zelda binding peaks and contained clusters of Zelda binding sites (limited to eight CAGGTAG and related sites; Nien et al., 2011). DNA fragments were amplified using *wt* genomic DNA as template and the Expand High Fidelity PCR System (Roche). Forward primers for amplification of candidate enhancers contain *Bgl*II (or *Bam*HI) restriction sites and reverse primers contain *Asc*I restriction sites. Amplified fragments were digested with *Bgl*II (or *Bam*HI) and *Asc*I and inserted into the piB-HC-*lacZ* vector (Chen et al., 2012a). Nucleotide changes in the Zelda binding sites were introduced by PCR mutagenesis. Primer sets are listed in supplementary material Table S2. Constructs were injected into embryos carrying the 38F1 landing site (Bateman et al., 2006; Bischof et al., 2007) to generate transgenic flies. At least three transformant lines for each construct were analyzed.

RNA probes and *in situ* hybridization

Primers for miRNA probe design are listed in supplementary material Table S2. *In situ* hybridization was performed as previously described (Liang et al., 2008; Nien et al., 2011). Embryos were stained with DAPI (1 mg/ml; Sigma-Aldrich) following hybridization.

Confocal image acquisition and image processing

Fluorescence *in situ* hybridization (FISH) images were acquired using a Leica TCS SP5 confocal microscope. *z*-sections containing pixel intensities higher than the median intensity of all pixels were selected for analysis. For each position in the *x-y* plane, the pixel with the strongest intensity across all *z*-sections was defined as the intensity value for that *x-y* position. All *z*-sections from the DAPI channel were processed to generate clear images of nuclei by customized Matlab scripts (Nien et al., 2011). Every FISH signal was assigned to the closest nucleus, when the distance between a FISH signal and the center of a nucleus was less than 1.5× the radius of the nucleus. The assigned nuclei were considered to show expression and were pseudocolored. Images were then further prepared using ImageJ (Abramoff et al., 2004).

miRNA target prediction

PicTar/doRiNA (Grün et al., 2005; Anders et al., 2012) and TargetScanFly (Ruby et al., 2007) were used for miRNA target predictions.

Acknowledgements

We thank Nicholas Sokol for the $miR\text{-}1^{KO}$ fly stock; Fen-Biao Gao for $miR\text{-}9a^{E39}$; Steve Small for bcd^{E1} and the piB-HC-*lacZ* vector; Eric Lai for the *UAS-miRNA* lines; Bomyi Lim for the *miR-2a-1* RNA probe; Kris Gunsalus for helpful discussions regarding miRNA targets; Nikolai Kirov and Yujia Sun for many insightful discussions and comments on the manuscript; and Josephine DeLuca and Utkarsh Patel for help with the transgenic studies.

Competing interests

The authors declare no competing financial interests.

Author contributions

S.F. and C.R. designed the experiments and prepared the manuscript. S.F. performed the transgenic reporter assays and genetic experiments. C.-Y.N. and H.-L.L. analyzed the expression profiling data. C.-Y.N. processed the FISH data for false coloring.

Funding

This work was supported by a grant from the National Institutes of Health [GM63024]. Deposited in PMC for release after 12 months.

Supplementary material

Supplementary material available online at
http://dev.biologists.org/lookup/suppl/doi:10.1242/dev.108118/-/DC1

References

Aboobaker, A. A., Tomancak, P., Patel, N., Rubin, G. M. and Lai, E. C. (2005). *Drosophila* microRNAs exhibit diverse spatial expression patterns during embryonic development. *Proc. Natl. Acad. Sci. U.S.A.* **102**, 18017-18022.

Abramoff, M. D. M., Paulo, J. and Ram, S. J. (2004). Image processing with ImageJ. *Biophotonics Int.* **11**, 36-42.

Ameres, S. L. and Zamore, P. D. (2013). Diversifying microRNA sequence and function. *Nat. Rev. Mol. Cell Biol.* **14**, 475-488.

Anders, G., Mackowiak, S. D., Jens, M., Maaskola, J., Kuntzagk, A., Rajewsky, N., Landthaler, M. and Dieterich, C. (2012). doRiNA: a database of RNA interactions in post-transcriptional regulation. *Nucleic Acids Res.* **40**, D180-D186.

Aravin, A. A., Lagos-Quintana, M., Yalcin, A., Zavolan, M., Marks, D., Snyder, B., Gaasterland, T., Meyer, J. and Tuschl, T. (2003). The small RNA profile during *Drosophila melanogaster* development. *Dev. Cell* **5**, 337-350.

Barrett, K., Leptin, M. and Settleman, J. (1997). The Rho GTPase and a putative RhoGEF mediate a signaling pathway for the cell shape changes in Drosophila gastrulation. *Cell* **91**, 905-915.

Bartel, D. P. (2004). MicroRNAs: genomics, biogenesis, mechanism, and function. *Cell* **116**, 281-297.

Bartel, D. P. (2009). MicroRNAs: target recognition and regulatory functions. *Cell* **136**, 215-233.

Bashirullah, A., Halsell, S. R., Cooperstock, R. L., Kloc, M., Karaiskakis, A., Fisher, W. W., Fu, W., Hamilton, J. K., Etkin, L. D. and Lipshitz, H. D. (1999). Joint action of two RNA degradation pathways controls the timing of maternal transcript elimination at the midblastula transition in *Drosophila melanogaster*. *EMBO J.* **18**, 2610-2620.

Bateman, J. R., Lee, A. M. and Wu, C.-t. (2006). Site-specific transformation of *Drosophila* via φC31 integrase-mediated cassette exchange. *Genetics* **173**, 769-777.

Bejarano, F., Bortolamiol-Becet, D., Dai, Q., Sun, K., Saj, A., Chou, Y.-T., Raleigh, D. R., Kim, K., Ni, J.-Q., Duan, H. et al. (2012). A genome-wide transgenic resource for conditional expression of *Drosophila* microRNAs. *Development* **139**, 2821-2831.

Bender, W. (2008). MicroRNAs in the *Drosophila* bithorax complex. *Genes Dev.* **22**, 14-19.

Berezikov, E., Cuppen, E. and Plasterk, R. H. A. (2006). Approaches to microRNA discovery. *Nat. Genet.* **38**, S2-S7.

Berezikov, E., Robine, E., Samsonova, A., Westholm, J. O., Naqvi, A., Hung, J.-H., Okamura, K., Dai, Q., Bortolamiol-Becat, D., Martin, R. et al. (2011). Deep annotation of *Drosophila melanogaster* microRNAs yields insights into their processing, modification, and emergence. *Genome Res.* **21**, 203-215.

Biemar, F., Zinzen, R., Ronshaugen, M., Sementchenko, V., Manak, J. R. and Levine, M. S. (2005). Spatial regulation of microRNA gene expression in the *Drosophila* embryo. *Proc. Natl. Acad. Sci. U.S.A.* **102**, 15907-15911.

Bischof, J., Maeda, R. K., Hediger, M., Karch, F. and Basler, K. (2007). An optimized transgenesis system for *Drosophila* using germ-line-specific φC31 integrases. *Proc. Natl. Acad. Sci. U.S.A.* **104**, 3312-3317.

Bosch, J. R. t., Benavides, J. A. and Cline, T. W. (2006). The TAGteam DNA motif controls the timing of *Drosophila* pre-blastoderm transcription. *Development* **133**, 1967-1977.

Boulay, J. L., Dennefeld, C. and Alberga, A. (1987). The *Drosophila* developmental gene *snail* encodes a protein with nucleic acid binding fingers. *Nature* **330**, 395-398.

Brenner, J. L., Jasiewicz, K. L., Fahley, A. F., Kemp, B. J. and Abbott, A. L. (2010). Loss of individual microRNAs causes mutant phenotypes in sensitized genetic backgrounds in *C. elegans*. *Curr. Biol.* **20**, 1321-1325.

Bushati, N., Stark, A., Brennecke, J. and Cohen, S. M. (2008). Temporal reciprocity of miRNAs and their targets during the maternal-to-zygotic transition in *Drosophila*. *Curr. Biol.* **18**, 501-506.

Carrington, J. C. and Ambros, V. (2003). Role of microRNAs in plant and animal development. *Science* **301**, 336-338.

Chen, H., Xu, Z., Mei, C., Yu, D. and Small, S. (2012a). A system of repressor gradients spatially organizes the boundaries of Bicoid-dependent target genes. *Cell* **149**, 618-629.

Chen, Z., Liang, S., Zhao, Y. and Han, Z. (2012b). miR-92b regulates Mef2 levels through a negative-feedback circuit during *Drosophila* muscle development. *Development* **139**, 3543-3552.

De Renzis, S., Elemento, O., Travzoie, S. and Wieschaus, E. F. (2007). Unmasking activation of the zygotic genome using chromosomal deletions in the *Drosophila* embryos. *PLoS Biol.* **5**, e117.

Flynt, A. S. and Lai, E. C. (2008). Biological principles of microRNA-mediated regulation: shared themes amid diversity. *Nat. Rev. Genet.* **9**, 831-842.

Ge, W., Chen, Y.-W., Weng, R., Lim, S. F., Buescher, M., Zhang, R. and Cohen, S. M. (2012). Overlapping functions of microRNAs in control of apoptosis during *Drosophila* embryogenesis. *Cell Death Differ.* **19**, 839-846.

Gellon, G. and McGinnis, W. (1998). Shaping animal body plans in development and evolution by modulation of Hox expression patterns. *BioEssays* **20**, 116-125.

Giraldez, A. J. (2010). MicroRNAs, the cell's Nepenthe: clearing the past during the maternal-to-zygotic transition and cellular reprogramming. *Curr. Opin. Genet. Dev.* **20**, 369-375.

Graveley, B. R., Brooks, A. N., Carison, J. W., Duff, M. O., Landolin, J. M., Yang, L., Artieri, C. G., van Baren, M. J., Boley, N., Booth, B. W. et al. (2011). The developmental transcriptome of *Drosophila melanogaster*. *Nature* **471**, 473-479.

Grün, D., Wang, Y.-L., Langenberger, D., Gunsalus, K. C. and Rajewsky, N. (2005). microRNA target predictions across seven *Drosophila* species and comparison to mammalian targets. *PLoS Comput. Biol.* **1**, e13.

Gummalla, M., Maeda, R. K., Castro Alvarez, J. J., Gyurkovics, H., Singari, S., Edwards, K. A., Karch, F. and Bender, W. (2012). *abd-A* regulation by the *iab-8* noncoding RNA. *PLoS Genet.* **8**, e1002720.

Harrison, M. M., Li, X.-Y., Kaplan, T., Botchan, M. R. and Eisen, M. B. (2011). Zelda binding in the early *Drosophila melanogaster* embryo marks regions subsequently activated at the maternal-to-zygotic transition. *PLoS Genet.* **7**, e1002266.

He, L. and Hannon, G. J. (2004). MicroRNAs: small RNAs with a big role in gene regulation. *Nat. Rev. Genet.* **5**, 522-531.

Hülskamp, M., Pfeifle, C. and Tautz, D. (1990). A morphogenetic gradient of *hunchback* protein organizes the expression of the gap genes *Krüppel* and *knirps* in the early *Drosophila* embryo. *Nature* **346**, 577-580.

Kanodia, J. S., Liang, H.-L., Kim, Y., Lim, B., Zhan, M., Lu, H., Rushlow, C. A. and Shvartsman, S. Y. (2012). Pattern formation by graded and uniform signals in the early *Drosophila* embryo. *Biophys. J.* **102**, 427-433.

Kosman, D., Ip, Y., Levine, M. and Arora, K. (1991). Establishment of the mesoderm-neuroectoderm boundary in the *Drosophila* embryo. *Science* **254**, 118-122.

Kozomara, A. and Griffiths-Jones, S. (2011). miRBase: integrating microRNA annotation and deep-sequencing data. *Nucleic Acids Res.* **39**, D152-D157.

Leaman, D., Chen, P. Y., Fak, J., Yalcin, A., Pearce, M., Unnerstall, U., Marks, D. S., Sander, C., Tuschl, T. and Gaul, U. (2005). Antisense-mediated depletion reveals essential and specific functions of microRNAs in *Drosophila* development. *Cell* **121**, 1097-1108.

Lee, R. C., Feinbaum, R. L. and Ambros, V. (1993). The *C. elegans* heterochronic gene *lin-4* encodes small RNAs with antisense complementarity to *lin-14*. *Cell* **75**, 843-854.

Lemons, D., Paré, A. and McGinnis, W. (2012). Three Drosophila Hox complex microRNAs do not have major effects on expression of evolutionarily conserved Hox gene targets during embryogenesis. *PLoS ONE* **7**, e31365.

Leptin, M. (1991). *twist* and *snail* as positive and negative regulators during *Drosophila* mesoderm development. *Genes Dev.* **5**, 1568-1576.

Li, Y., Wang, F., Lee, J.-A. and Gao, F.-B. (2006). MicroRNA-9a ensures the precise specification of sensory organ precursors in *Drosophila*. *Genes Dev.* **20**, 793-2805.

Liang, H.-L., Nien, C.-Y., Liu, H.-Y., Metzstein, M. M., Kirov, N. and Rushlow, C. (2008). The zinc-finger protein Zelda is a key activator of the early zygotic genome in *Drosophila*. *Nature* **456**, 400-403.

Martinez, N. J. and Walhout, A. J. M. (2009). The interplay between transcription factors and microRNAs in genome-scale regulatory networks. *BioEssays* **31**, 435-445.

McGinnis, W. and Krumlauf, R. (1992). Homeobox genes and axial patterning. *Cell* **68**, 283-302.

Mendell, J. T. and Olson, E. N. (2012). MicroRNAs in stress signaling and human disease. *Cell* **148**, 1172-1187.

Nicol, J. W., Helt, G. A., Blanchard, S. G., Raja, A. and Loraine, A. E. (2009). The Integrated Genome Browser: free software for distribution and exploration of genome-scale datasets. *Bioinformatics* **25**, 2730-2731.

Nien, C.-Y., Liang, H.-L., Butcher, S., Sun, Y., Fu, S., Gocha, T., Kirov, N., Manak, J. R. and Rushlow, C. (2011). Temporal coordination of gene networks by Zelda in the early *Drosophila* embryo. *PLoS Genet.* **7**, e1002339.

Ochoa-Espinosa, A., Yu, D., Tsirigos, A., Struffi, P. and Small, S. (2009). Anterior-posterior positional information in the absence of a strong Bicoid gradient. *Proc. Natl. Acad. Sci. U.S.A.* **106**, 3823-3828.

Ozsolak, F., Poling, L. L., Wang, Z., Liu, H., Liu, X. S., Roeder, R. G., Zhang, X., Song, J. S. and Fisher, D. E. (2008). Chromatin structure analyses identify miRNA promoters. *Genes Dev.* **22**, 3172-3183.

Papatsenko, D. (2007). ClusterDraw web server: a tool to identify and visualize clusters of binding motifs for transcription factors. *Bioinformatics* **23**, 1032-1034.
Perry, M. W., Boettiger, A. N., Bothma, J. P. and Levine, M. (2010). Shadow enhancers foster robustness of *Drosophila* gastrulation. *Curr. Biol.* **20**, 1562-1567.
Perry, M. W., Boettiger, A. N. and Levine, M. (2011). Multiple enhancers ensure precision of gap gene-expression patterns in the *Drosophila* embryo. *Proc. Natl. Acad. Sci. U.S.A.* **108**, 13570-13575.
Petruk, S., Sedkov, Y., Riley, K. M., Hodgson, J., Schweisguth, F., Hirose, S., Jaynes, J. B., Brock, H. W. and Mazo, A. (2006). Transcription of *bxd* noncoding-RNAs promoted by *Trithorax* represses *Ubx* in *cis* by transcriptional interference. *Cell* **127**, 1209-1221.
Qian, J., Zhang, Z., Liang, J., Ge, Q., Duan, X., Ma, F. and Li, F. (2011). The full-length transcripts and promoter analysis of intergenic microRNAs in *Drosophila melanogaster*. *Genomics* **97**, 294-303.
Rajewsky, N. (2006). MicroRNA target predictions in animals. *Nat. Genet.* **38**, S8-S13.
Ronshaugen, M., Biemar, F., Piel, J., Levine, M. and Lai, E. C. (2005). The *Drosophila* microRNA *iab-4* causes a dominant homeotic transformation of halteres to wings. *Genes Dev.* **19**, 2947-2952.
Ruby, J. G., Stark, A., Johnston, W. K., Kellis, M., Bartel, D. P. and Lai, E. C. (2007). Evolution, biogenesis, expression, and target predictions of a substantially expanded set of *Drosophila* microRNAs. *Genome Res.* **17**, 1850-1864.
Sanny, J., Chui, V., Langmann, C., Pereira, C., Zahedi, B. and Harden, N. (2006). Drosophila RhoGAP68F is a putative GTPase activating protein for RhoA participating in gastrulation. *Dev. Genes Evol.* **216**, 543-550.
Schier, A. F. (2007). The maternal-zygotic transition: death and birth of RNAs. *Science* **316**, 406-407.
Sempere, L. F., Sokol, N. S., Dubrovsky, E. B., Berger, E. M. and Ambros, V. (2003). Temporal regulation of microRNAs expression in *Drosophila melanogaster* mediated by hormonal signals and Broad-Complex gene activity. *Dev. Biol.* **259**, 9-18.
Smibert, P. and Lai, E. C. (2008). Lessons from microRNA mutants in worms, flies and mice. *Cell Cycle* **7**, 2500-2508.
Sokol, N. (2008). An overview of the identification, detection, and functional analysis of *Drosophila* microRNAs. In *Drosophila: Methods and Protocols* (ed. C. Dahmann), pp. 319-334. Totowa, NJ: Humana Press.
Sokol, N. S. and Ambros, V. (2005). Mesodermally expressed *Drosophila* microRNA-1 is regulated by Twist and is required in muscles during larval growth. *Genes Dev.* **19**, 2343-2354.
Stark, A., Bushati, N., Jan, C. H., Kheradpour, P., Hodges, E., Brennecke, J., Bartel, D. P., Cohen, S. M. and Kellis, M. (2008). A single Hox locus in *Drosophila* produces functional microRNAs from opposite DNA strands. *Genes Dev.* **22**, 8-13.
Tadros, W. and Lipshitz, H. D. (2009). The maternal-to-zygotic transition: a play in two acts. *Development* **136**, 3033-3042.
Tadros, W., Goldman, A. L., Babak, T., Menzies, F., Vardy, L., Orr-Weaver, T., Hughes, T. R., Westwood, J. T., Smibert, C. A. and Lipshitz, H. D. (2007). SMAUG is a major regulator of maternal mRNA destabilization in *Drosophila* and its translation is activated by the PAN GU kinase. *Dev. Cell* **12**, 143-155.
The modENCODE Consortium, S. Roy, J. Ernst, P. V. Kharchenko, P. Kheradpour, N. Negre, M. L. Eaton, J. M. Landolin, C. A. Bristow, L. Ma et al. (2010). Identification of functional elements and regulatory circuits by *Drosophila* modENCODE. *Science* **330**, 1787-1797.
Thomsen, S., Anders, S., Janga, S. C., Huber, W. and Alonso, C. (2010). Genome-wide analysis of mRNA decay patterns during early *Drosophila* development. *Genome Biol.* **11**, R93.
Thomson, D. W., Bracken, C. P. and Goodall, G. J. (2011). Experimental strategies for microRNA target identification. *Nucleic Acids Res.* **39**, 6845-6853.
Truscott, M., Islam, A. B. M. M. K., Lopez-Bigas, N. and Frolov, M. V. (2011). MiR-11 limits the proapoptotic function of its host gene, *dE2f1*. *Genes Dev.* **25**, 1820-1834.
Tweedie, S., Ashburner, M., Falls, K., Leyland, P., McQuilton, P., Marygold, S., Millburn, G., Osumi-Sutherland, D., Schroeder, A., Seal, R. et al. (2009). FlyBase: enhancing *Drosophila* Gene Ontology annotations. *Nucleic Acids Res.* **37**, D555-D559.
Tyler, D. M., Okamura, K., Chung, W.-J., Hagen, J. W., Berezikov, E., Hannon, G. J. and Lai, E. C. (2008). Functionally distinct regulatory RNAs generated by bidirectional transcription and processing of microRNA loci. *Genes Dev.* **22**, 26-36.
Yekta, S., Tabin, C. J. and Bartel, D. P. (2008). MicroRNAs in the Hox network: an apparent link to posterior prevalence. *Nat. Rev. Genet.* **9**, 789-796.
Zeitlinger, J., Zinzen, R. P., Stark, A., Kellis, M., Zhang, H., Young, R. A. and Levine, M. (2007). Whole-genome ChIP-chip analysis of Dorsal, Twist, and Snail suggests integration of diverse patterning processes in the *Drosophila* embryo. *Genes Dev.* **21**, 385-390.

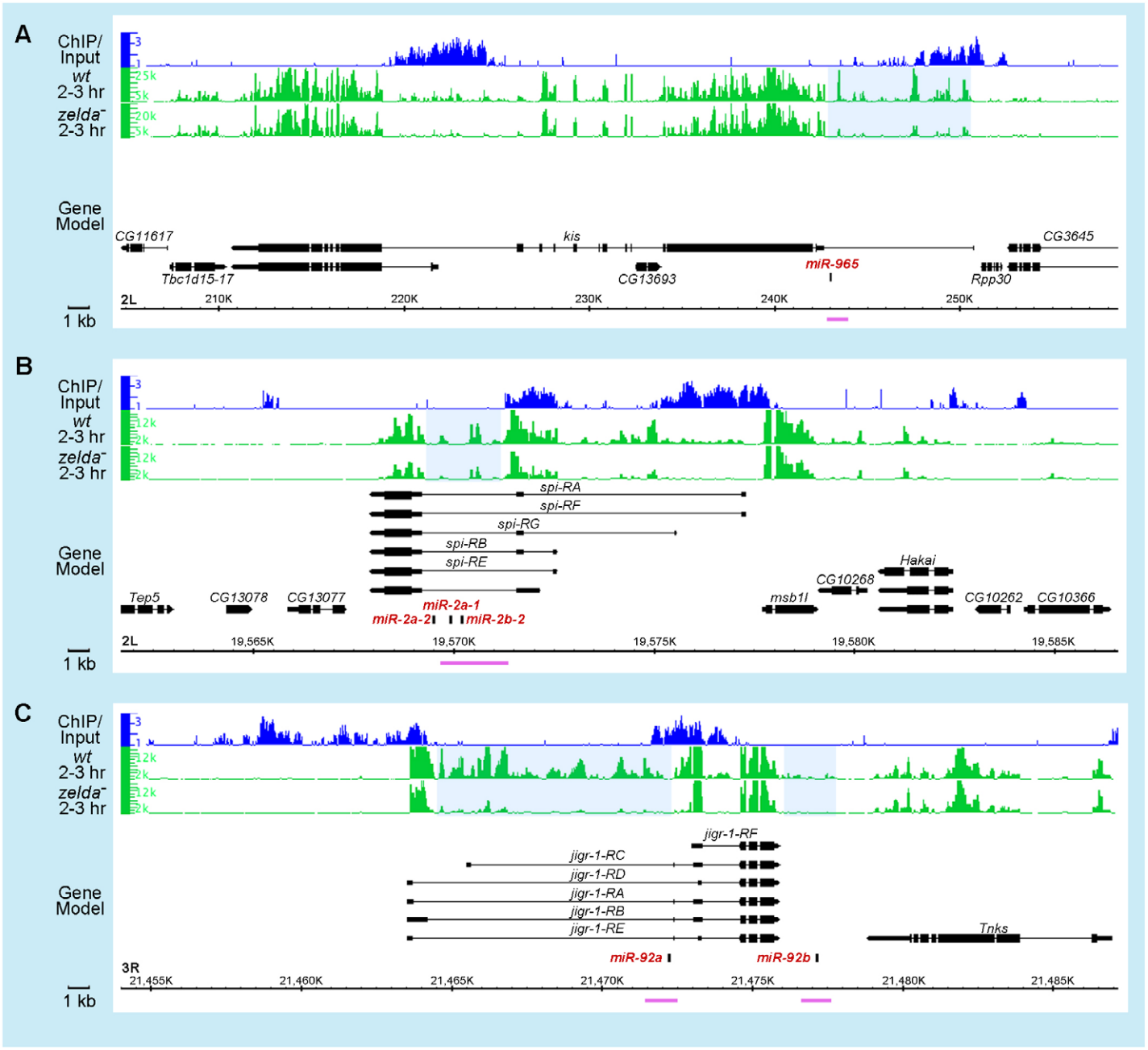

Fig. S1. Three of the early-expressed miRNAs reside in introns of other genes. Browser views of three intronic miRNA clusters: (A) *miR-965* in *kis*; (B) *miR-2a-1* cluster in *spi*; (C) *miR-92a* in *jigr-1* (see Fig. 1 legend for description of tracks).

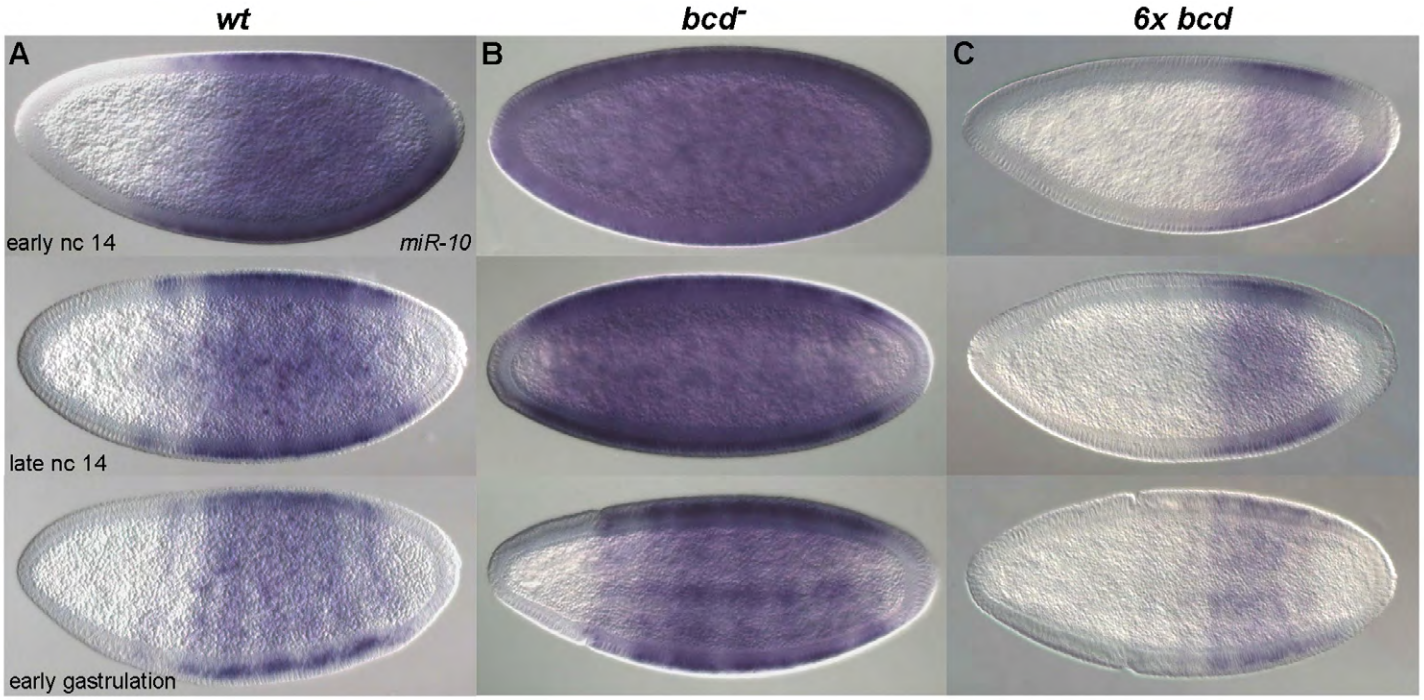

Fig. S2. The Bcd dependent pathway represses *miR-10*. Wild-type (*wt*, A), *bcd* mutant (B) and 6x *bcd* embryos (C) hybridized with RNA probes against *pri-miR-10*. In *wt*, *miR-10* is initially expressed in the posterior region (A, early nc 14). Later, as nc 14 progresses, *miR-10* expression refines into seven stripes along the AP axis. In *bcd* mutants, the onset time of *miR-10* expression is not affected (B, early nc 14), but it is detected uniformly across the entire embryo. Though the pattern refines later on, *miR-10* expression expands anteriorly (A, B, mid, late nc 14, and early gastrulation). In contrast, in 6x *bcd* embryos, the anterior repression of *miR-10* expands along with the expansion of the Bcd gradient (C).

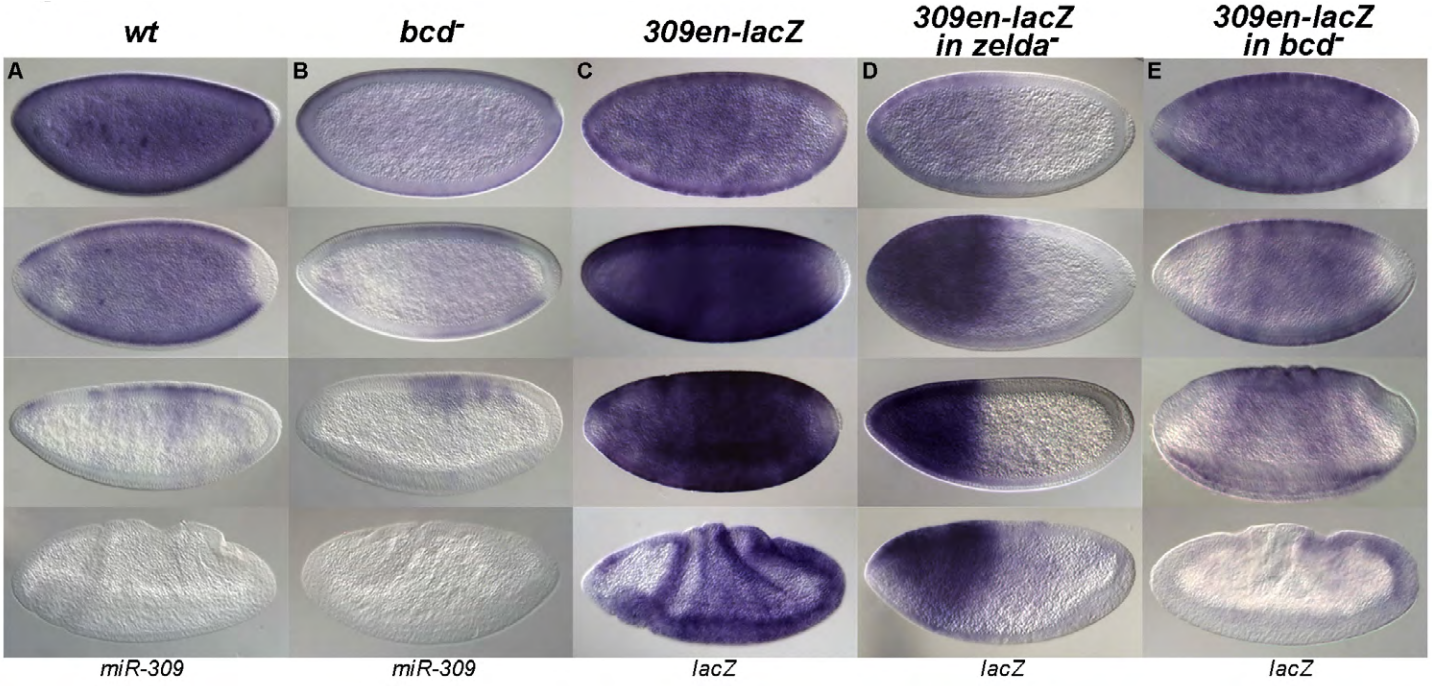

Fig. S3. The Bcd dependent pathway activates *miR-309*. Wild-type (*wt*, A, C), *bcd* mutant (B, E) and *zelda* mutant (D) embryos hybridized with RNA probes against *pri-miR-309* transcripts (A, B) or *lacZ* (C, D, E). In *wt*, *miR-309* is initially expressed throughout the entire embryo (A, early nc 14). Later, as nc 14 progresses, *miR-309* refines along both the A-P and D-V axes, as expression is lost in the ventral region and in stripes along A-P axis. In *bcd* mutants, the initial uniform expression of *miR-309* was not affected (B, early nc 14), but became restricted to the posterior region later on (B, late nc 14 and early gastrulation). *lacZ* driven by the *miR-309* enhancer is expressed ubiquitously in the embryo similar to endogenous *miR-309*, suggesting that this enhancer is responsible for *miR-309* activation (C). *lacZ* expression persists into germ band extension stages, indicating that this enhancer is lacking repression elements. In *zelda* mutants, only anterior *lacZ* expression is detected (D). In *bcd* mutants, anterior *lacZ* expression is reduced and eventually lost at the germ band extension stage (E).

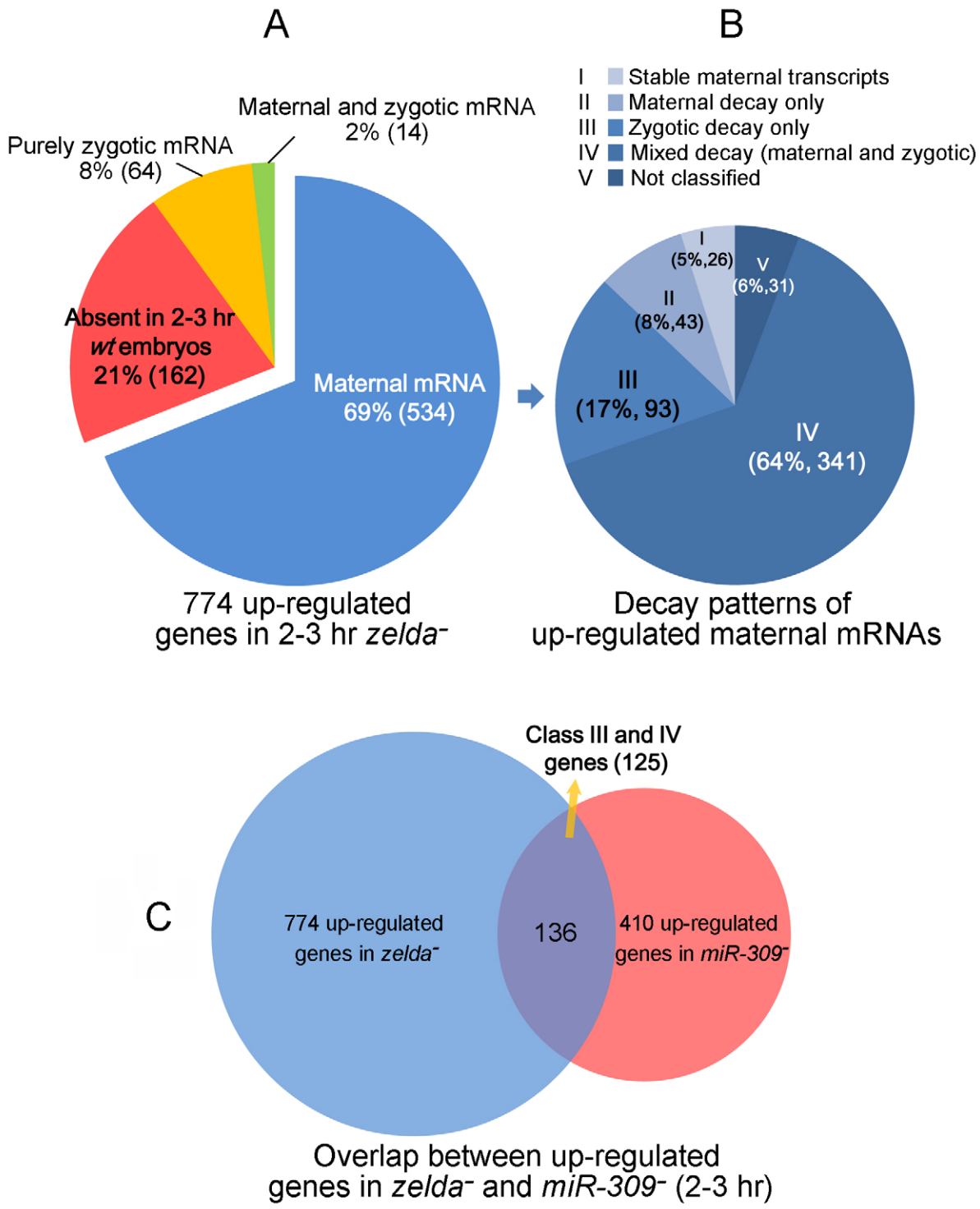

Fig. S4. Analysis of up-regulated genes in 2-3 hour *zelda* mutant embryos. (A) Pie chart showing proportion (and number of genes, Supplementary material Table S3) of the 774 up-regulated genes in *zelda* mutants in four categories: maternal mRNA (mRNAs preloaded into the embryo during oogenesis); maternal and zygotic mRNA (mRNAs preloaded and transcribed in the embryo); purely zygotic mRNA (mRNAs newly transcribed in the embryo); and absent (not detected in wild-type (*wt*), but up-regulated in *zelda* mutants). Note that 69% of the up-regulated genes are maternally loaded. (B) Pie chart showing the 534 maternal mRNAs from (A) in 5 categories based on their decay pattern during the MZT (from classification in Thomsen et al., 2010, Supplementary material Table S3). 89% (434) of the up-regulated maternal mRNAs in *zelda* mutants are unstable maternal mRNAs (Supplementary material Table S3), and are degraded either by maternal mRNA decay pathway only (II), or by zygotic mRNA decay pathway only (III), or by both (IV). (C) 136 of the 774 up-regulated genes in *zelda* mutants overlap with those up-regulated in *miR-309* mutants; of these, ~92% (125, Supplementary material Table S3) are type III and IV genes, indicating that the up-regulation of these genes in *zelda* mutants is due to the disruption of the mRNA decay pathway conducted by miR-309.

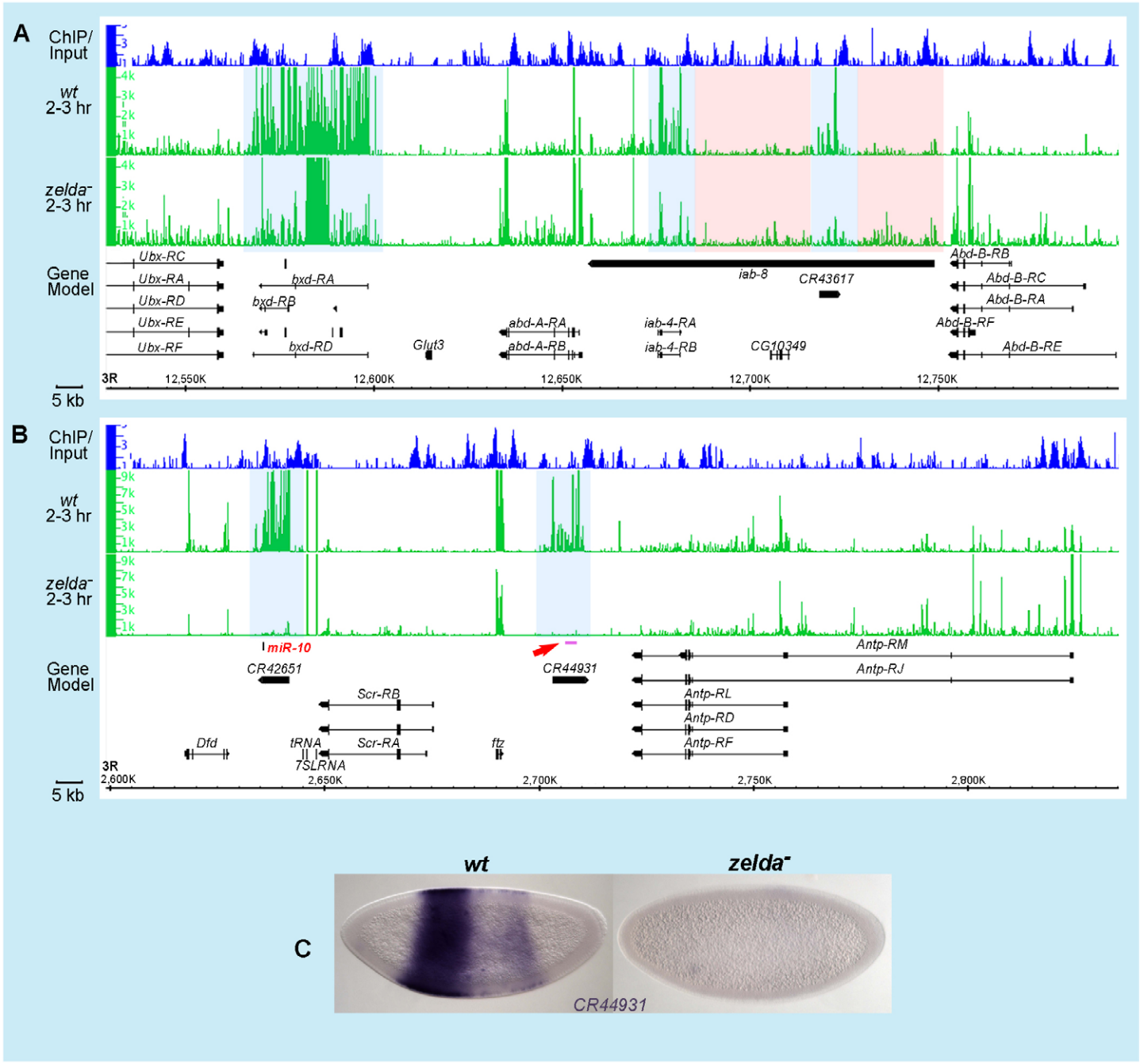

Fig. S5. MiRNAs and lincRNAs in the Hox gene complexes. Browser views of genomic regions spanning *Ubx* to *Abd-B* in the *Bithorax complex (BX-C)* (A) and *Dfd* to *Antp* in the *Antennapedia complex* (*ANT-C*) (B). Tracks above gene models are as described in Figures 1 and S1. Light blue shadowing in the expression tracks indicates regions down-regulated in *zelda* mutants. Light red shadowing indicates regions up-regulated in *zelda* mutants. (C) Wild-type (*wt*) and *zelda* mutant embryos hybridized with RNA probes against *CR44931* (purple line with red arrow in B). Note that *CR44931* is expressed in a broad central domain in *wt*, but is not detected in *zelda* mutants.

Table S1. miRNAs tested in this study

miRNA name	miRNA position	Host genes	RNA Probe location	Probe size (nt)	Expression in 0-6 hr embryos (previous literatures*)	Expression in 1-3 hr wild-type tiling array	Zelda binding within 2 kb of miRNA transcription units or host genes	Nuclei dots in wild-type 1-3 hr	MiRNA expression in *zelda*$^{-}$ compared to wild-type(1-3 hr)
miR-1	intergenic	n/a	2L: 20486777 -20488219	1443	yes	yes	yes	yes	Down-regulated
miR-10	intergenic	n/a	3R: 2634611 -2636419	1809	yes	yes	yes	yes	Down-regulated
miR-11	intronic	*E2f*	3R: 17447463 -17448432	970	yes	yes	yes	yes	Down-regulated
miR-309 cluster	intergenic	n/a	2R: 15548119 -15549170	1052	yes	yes	yes	yes	Down-regulated
miR-9a	intergenic	n/a	3L: 19556781 -19558851	2071	yes	yes	yes	yes	Down-regulated
miR-92a	intronic	*jigr1*	3R: 21471476 -21472485	1010	yes	yes	yes	yes	Down-regulated
miR-92b	intergenic	n/a	3R: 21476633 -21477659	1027	yes	yes	yes	yes	Down-regulated
miR-iab-4	intergenic	n/a	3R: 12681571 -12683390	1820	yes	yes	yes	yes	Down-regulated
miR-iab-4as	intergenic	n/a	3R: 12681571 -12683390	1820	yes	yes	yes	yes	Up-regulated
miR-965	intronic	*kis*	2L: 242854 -243924	1071	yes	yes	yes	yes	Down-regulated
miR-2a-1 cluster	intronic	*spi*	2L: 19569658 -19571349	1692	yes	yes	yes	yes	Down-regulated
miR-13a cluster	intergenic	n/a	3R: 11243042 -11244277	1237	yes	very low	yes	no	n/a
miR-2b-1	intergenic	n/a	2L: 8258046 -8259423	1378	yes	no	no	no	n/a
miR-14	intergenic	n/a	2R: 5440704 -5441997	1294	yes	no	low	no	n/a
miR-184	intergenic	n/a	2R: 9215877 -9217583	1707	yes	no	no	no	n/a

miR-310 cluster	intergenic	n/a	2R: 1647100 -16471924	925	yes	no	yes	no	n/a
miR-263a	intergenic	n/a	2L: 11952599 -11954372	1774	yes	no	no	no	n/a
miR-279	intergenic	n/a	3R: 25040758 -25042088	1331	yes	no	yes	no	n/a
miR-280	intergenic	n/a	2R: 4184860 -4186524	1665	yes	no	low	no	n/a
miR-281-1 cluster	intronic	*Oda*	2R: 8057551 -8058477	927	yes	no	yes	no	n/a
miR-287	intergenic	n/a	2L: 17574021 -17575419	1399	yes	no	no	no	n/a
miR-304 cluster	intronic	*Gmap*	X: 15401733 -15403640	1908	yes	no	low	no	n/a
miR-305 cluster	intergenic	n/a	2L: 7425191 -7426685	1495	yes	no	yes	no	n/a
miR-9c	intronic	*grp*	2L: 16697657 -16698096	440	yes	no	no	no	n/a
miR-306 cluster	intronic	*grp*	2L: 16698407 -16698892	486	yes	no	no	no	n/a
miR-307	intronic	*Mmp2*	2R: 5508113 -5509654	1542	yes	no	no	no	n/a
miR-308	intronic	*RpS23*	2R: 10103276 -10103406	131	yes	no	yes	no	n/a
miR-31a	intergenic	n/a	2R: 13670690 -13672263	1574	yes	no	yes	no	n/a
miR-31b	intergenic	n/a	X: 8886574 -8888275	1702	yes	no	no	no	n/a
miR-7	intronic	*bl*	2R: 16493354 -16493849	496	yes	no	yes	no	n/a
miR-8	intergenic	n/a	2R: 12718272 -12719620	1349	yes	no	yes	no	n/a

*Aravin et al., 2003; Ruby et al., 2007.

Table S2. Primer sequences

Primer sets	Primer name	Forward primers (5'>>3')	Reverse primers (5'>>3')
Probe	miR-1	TTTATTACGGGCAACCAACGACG	AGGGCTTACTGTGCTCCAACCG
	miR-10	TTGACTGCGTTTGTTTTATTTCC	GATTCGTCCTCCTTCCTTTGTTT
	miR-11	CAACCGATCATGCCTGCAACC	TAAATGTTCTGCAGTTCGGGGCT
	miR-309 cluster	CCGATCCTGGGATGCATCTTGTG	CCCAAATGTTCAAAGCTTGAG
	miR-9a	ATGGTACTGCGTGATAGGATTGA	CTTACTTTCCGAGTTTATGGTGTTT
	miR-92a	CAGCGATCAAATAAACAAATAC	TAAACAAGAAGCAAACTCACC
	miR-92b	TTGCTGATCGATGTTGTGGGACG	AGTGCGTCTCTTTTTCGGGCCTT
	miR-iab-4	GTCTTATGTGACAAGTGCTGGCTA	TCACCACCTCCTTCTCATCGTGCT
	miR-iab-4as	GTCTTATGTGACAAGTGCTGGCTA	TCACCACCTCCTTCTCATCGTGCT
	miR-965	TTTCGGTTTTGAGCGTATTT	CTTAGGGTGTAGAGGGGACG
	miR-13a cluster	ATCCTTATTCCTTCTCCGATTTTC	AGCGGCGGGAAGCACAGTTAGA
	miR-2a-1 cluster	TACTCCTTTCTTCACATCCAA	CTCTTTCAGTGTTGTTCTTCG
	miR-2b-1	GATTGTGGTTATGTAATGCGAGAC	ATGTTTGCGAGCCAAGTTCAGC
	miR-14	AGAAAAGAGGGAGACGGCATCA	CAGCAAAAGTCCCATGACAAAT
	miR-184	AAATATCATATCACCCTTGTAACCC	CAACATTGCCACTTGAAATCCAC
	miR-310 cluster	TTGTTGCACCAGTTGTACGGGAAT	ACAAAACTGGCATTCCCGTCTTACT
	miR-263a	TTGAAGCGTTTAGCGTTGGA	CCTCGGCGGAAATTACCAAC
	miR-279	ACAACAAGAGGGCAAGACATA	GAGGCGGAACTACAGAGGAAT
	miR-280	GTCGGGCGGAGGATGGTTAT	GGCTTAGGGTCTTCGGTGGG
	miR-281-1 cluster	TGAAAGGTGGGAAGGGATTAGA	CGCAGCCAGATAACCAGAAGAT
	miR-287	AGCCCTTTACCGCAACTTATA	ATTATCCTGTCATGGGTCCTG
	miR-304 cluster	AACCTATTGAAGCACCTCCG	CACATCCGTTTGGGTGAAGC
	miR-305 cluster	CAAGGGTCTGCCGAACGAAACG	GCATGGGAATGAGTGCGGTGAG

Probe	miR-9c	CGGTGCGAGATTGTTTTACATGTG	TTTGCAAGCACAGACGAAGAATTACA
	miR-306 cluster	CACTCGATGGCTCAGGTACTTAG	TGAGAACAAGTAACGCGAGAAAAG
	miR-307	CATCAGACAGACGACCGACAC	ATCCAGCTCATTCCCTACTCC
	miR-308	CGGATGAGATGGCGGGGTTAA	AGTCGCTTTTCGCTGCTGGCA
	miR-31a	TGGGTTTGCAGCAATTAAGGC	TTCCGAAACGACAACGACTGG
	miR-31b	TTGAGACGATGAACGCACTG	CGCTAAATACTTGTCGCAATAAAC
	miR-7	GAGGTTGGTGTCGCAATCTGAATA	ATGTGGATGTAGTGGGATGGGAGG
	miR-8	GGCGTTATTGTGCATGTTTCC	ACCTGCTGTCTTGGCTAGTTG
	fog-exon3	CCTGCTGATTCCGTACTTGCT	ATTGTCTGCTGGCTGTTCTGG
	fog-intron1	CGGAGAACTATGAGTAGGGACG	GAAGTGATTGCTGTGAGGGTG
Enhancers tested	miR-1-0.6kb enhancer	GAAGATCTGTCATATGATTGGAGGAAGACTC	TTGGCGCGCCATCTTCGAGTGCAGTGTGCATCTACGA
	miR-1-0.6kb TAG m1	CATAGTTCTGAACGCTCGAGAACTGACATTATTCCG	CGGAATAATGTCAGTTCTCGAGCGTTCAGAACTATG
	miR-1-0.6kb TAG m2	CTTAGTGAGCAAGTCGACAGCCGAGTGTGCTGGCT	AGCCAGCACACTCGGCTGTCGACTTGCTCACTAAG
	miR-9a enhancer I (9a-I)	CGGGATCCTTTGATTACGACGAGGGTCAGG	TTGGCGCGCCAGACGTGGAATGGGAACAAGAT
	miR-9a enhancer II (9a-II)	CGGGATCCTTATAGAGGAGCAAGATACCCG	TTGGCGCGCCATATGAGATGAGGCAGATGACG
	9a-IIm1	CCTCTAGATGTCTTATATGTGTGCCTCTCATTTG	ACATCTAGAGGGTAGGAGACAAGTACAAAGC
	9a-IIm2	TCACTAGTCAACGCTGCCGGCGTCGCAGTCGGCGCTACATATGAG	TTGACTAGTGATTTTCGGGTTTTTGTTTTTGCC
	miR-10 enhancer (10-en)	GAAGATCTTCATGTCAACCCCATCGCAGCA	TTGGCGCGCCAAGCCGGTAATGTTCTCCCTCA
	DNA fragment within miR-10	GATAGATCTGCCCATGGGCGAGG	TTGGCGCGCCTTCCGCTCATTGAACCAGTA
	miR-iab-4 enhancer (iab-en)	GAAGATCTCTATGCTGCTTCCCAAGTGCCA	TTGGCGCGCCTGCAATTCCAGCGAAGGACAAC
	DNA fragment upstream miR-iab-4	GAAGATCTGAAGACTGGCAGACAAATAAACA	TTGGCGCGCCAATGGTATTGGGATTCAAGGAC
	DNA fragment downstream miR-iab-4	GAAGATCTGACCGTGGGACCAGATGGATG	TTGGCGCGCCTTAAACCTCGGCGGGCCTAAA
	miR-11 enhancer (11-en)	CGGGATCCTGCTGGAACATACCATCGA	TTGGCGCGCCCATTTGGGCAGTGTCCTTT
	DNA fragment near miR-92a	CGGGATCCTCAGAAACTCCCACTCCTC	TTGGCGCGCCATTGGACTTCGGACAGGTA

Table S3. Analysis of the 774 upregulated genes in 2-3 h zelda mutants.
Download Table S3